



Contents lists available at ScienceDirect

## Arabian Journal of Chemistry

journal homepage: [www.ksu.edu.sa](http://www.ksu.edu.sa)

Review article

## *In vivo* wound healing activity of electrospun nanofibers embedding natural products



Breno de Almeida Bertassoni<sup>a,b</sup>, Denise de Abreu Garófalo<sup>b</sup>,  
 Mariana Sato de Souza Bustamante Monteiro<sup>b</sup>, Ralph Santos-Oliveira<sup>c</sup>,  
 Anne Caroline Candido Gomes<sup>d</sup>, Anna Leticia Martinez Martinez Toledo<sup>e</sup>, Marcos Lopes Dias<sup>e</sup>,  
 Naomi Kato Simas<sup>b</sup>, Eduardo Ricci-Junior<sup>a,\*</sup>

<sup>a</sup> Natural Products and Biological Assays Laboratory, Natural and Food Products Department, Pharmacy School, Federal University of Rio de Janeiro (Universidade Federal do Rio de Janeiro, UFRJ), 21941-902 Rio de Janeiro, Brazil

<sup>b</sup> Pharmaceutical Nanotechnology Laboratory, Pharmacy School, Federal University of Rio de Janeiro (Universidade Federal do Rio de Janeiro, UFRJ), 21941-901 Rio de Janeiro, Brazil

<sup>c</sup> Nanoradiopharmacy and Synthesis of Novel Radiopharmaceuticals Laboratory, Nuclear Engineering Institute, Brazilian Nuclear Energy Commission, Rio de Janeiro 21941906, RJ, Brazil

<sup>d</sup> Rio de Janeiro Education, Science and Technology Federal Institute (Instituto Federal de Educação, Ciência e Tecnologia do Rio de Janeiro, IFRJ), 21715-000 Rio de Janeiro, Brazil

<sup>e</sup> Professor Eloisa Mano Macromolecules Institute (Instituto de Macromoléculas, IMA), Federal University of Rio de Janeiro, Rio de Janeiro, Brazil

## ARTICLE INFO

## Keyword:

Nanofibrous scaffolds  
 Electrospinning  
 Natural products  
 Wound dressings  
 Plant extracts

## ABSTRACT

Nanofibers are threads at the nanometric scale. Electrospinning is a technique that uses electric fields as the driving force to produce fibers ranging from nanometers to micrometers. Membranes based on polymeric nanofibers obtained through electrospinning possess an excellent capacity to carry drugs and natural active components, promoting skin healing and regeneration in various ways. Natural products derived from plants have gained attention in recent decades due to their accessibility, good biocompatibility, biodegradability, and incorporation into nanofibers. These products can influence multiple stages of the healing process and exhibit antimicrobial activity, thereby preventing and combating infections. Consequently, the combination of natural products and nanofibers presents a promising approach to infection prevention and skin wound healing. In this context, the current paper presents a systematic literature review of studies conducted from 2011 to 2024. It focuses on articles concerning the production of nanofibers via electrospinning that embed active components of natural origin, specifically those that performed *in vivo* tests to assess wound healing potential. A total of 26 articles met the inclusion criteria and were analyzed in terms of production and characterization of the electrospun membranes using *in vitro* and *in vivo* tests. Most studies employed a mixture of polyvinyl alcohol (PVA) with another polymer, utilized plant extracts like *Malva sylvestris* as active components, and performed *in vitro* tests using fibroblasts. Antimicrobial tests were conducted against *Staphylococcus aureus* and *Escherichia coli*, while male Wistar rats were used in excision/incision wound models for *in vivo* tests. The results indicate that natural products influence the properties of the scaffolds in different ways, such as increasing fiber diameter and mechanical strength, and may also accelerate wound healing.

## 1. Introduction

Polymeric nanofibers are threads at the nanometric scale, composed of natural and/or synthetic polymers, and produced by various techniques, with electrospinning standing out among them (Berthet et al.,

2017; Blanco-Fernandez et al., 2021). Nanofibrous membranes serve as a physical barrier that isolates wounds from external microorganisms and contaminants (Croitoru et al., 2020; Hajialyani et al., 2018). Their porous structure facilitates gas exchange and maintains adequate humidity at the wound site while allowing absorption of exudates.

\* Corresponding author at: Pharmaceutical Nanotechnology Laboratory, Pharmacy School, Federal University of Rio de Janeiro (UFRJ), 21941-901 Rio de Janeiro, Brazil.

E-mail address: [ricci@pharma.ufrj.br](mailto:ricci@pharma.ufrj.br) (E. Ricci-Junior).

<https://doi.org/10.1016/j.arabjc.2024.106019>

Received 13 May 2024; Accepted 8 October 2024

Available online 15 October 2024

1878-5352/© 2024 The Author(s). Published by Elsevier B.V. on behalf of King Saud University. This is an open access article under the CC BY-NC-ND license (<http://creativecommons.org/licenses/by-nc-nd/4.0/>).

Additionally, these membranes can incorporate natural extracts and active substances, which favor prolonged release and enhance tissue regeneration (Berthet et al., 2017; Croitoru et al., 2020; Dias et al., 2016; Hajjalyani et al., 2018). The nanometric size of these fibers also promotes the adhesion and proliferation of fibroblasts and keratinocytes, thereby contributing to tissue healing and regeneration (Berthet et al., 2017; Croitoru et al., 2020; Dias et al., 2016; Hajjalyani et al., 2018). Furthermore, the potential to reduce the frequency of dressing exchanges enhances patient comfort and decreases treatment costs (Ambekar & Kandasubramanian, 2019). Moreover, combining electrospun membranes with different formulations results in composite scaffolds that offer additional advantages, such as increased hydrophilicity and water absorption capacity, when combined with hydrogels (Meng et al., 2024).

Electrospinning is a widely used technique due to its low cost and ability to produce fibers of varying diameters (3 nm–6  $\mu\text{m}$ ) that can carry active components, enabling modified release of these substances. Its versatility extends to various natural and synthetic polymers (Croitoru et al., 2020; Dias et al., 2016). The process involves dissolving a polymer in a suitable solvent to create a polymeric solution, which is placed in a syringe with the nozzle pointed toward a collector (either static or mobile, such as a cylinder or rotating tray). A high voltage generates an electrostatic field between the syringe and the collector, allowing the solution to be expelled with a pump at a controlled flow rate. As the drop is attracted and stretched from the syringe nozzle to the collector, the solvent evaporates, forming fibers (Fig. 1) (Croitoru et al., 2020; Dias et al., 2016; Li et al., 2023). The polarity of the syringe depends on the chemical nature of the polymer: for negatively charged polymers, the syringe is negatively charged while the collector is positive, and vice versa (Croitoru et al., 2020).

Another method, coaxial electrospinning, utilizes two or more aligned concentric needles. In this setup, a polymeric solution containing the active substance is expelled through the inner needle, while another polymeric solution is expelled through the outer needle, creating a 'core-shell' fiber system (Croitoru et al., 2020; Dias et al., 2016). Electrospinning emulsions can also create 'core-shell' systems without requiring a coaxial needle system. In this case, the dispersed phase of the emulsion serves as the inner phase (core), while the continuous phase acts as the outer phase (shell) (Dias et al., 2016). 'Core-shell' membranes protect the active substances in the inner layer from the external environment and modulate their release (Croitoru et al., 2020; Dias et al., 2016). Furthermore, electrospinning techniques can be combined with traditional textile methods, leading to new nanometric scaffolds known as 'nanofiber yarns,' which can be utilized for biomedical applications (Wu et al., 2022).

Several parameters can influence the final morphology of the fibers.

For example, factors like fiber orientation (aligned or not), morphology, and uniformity (continuous fibers or those with polymeric clusters) can be controlled by adjusting the viscosity and electrical conductivity of the solution, as well as temperature, humidity, pressure, polymer concentration, flow rate, distance from the syringe to the collector, and collector rotation (Croitoru et al., 2020; Dias et al., 2016).

Characterization of electrospun membranes requires the use of various techniques and devices. Microscopy methods, such as scanning electron microscopy (SEM), transmission electron microscopy (TEM), and atomic force microscopy (AFM), are employed to evaluate the morphology, porosity, diameter, and orientation of the fibers. Crystallinity can be assessed through X-ray diffraction (XRD), while chemical composition is typically analyzed using Fourier transform infrared (FTIR) spectroscopy or nuclear magnetic resonance (NMR). The surface chemical composition can be determined by measuring the contact angle with water or using FTIR with attenuated total reflection (ATR). Additionally, the thermal stability, degradation, compatibility, and interaction of the polymer with the active component can be investigated using thermogravimetric analysis (TGA) and differential scanning calorimetry (DSC) (Bhardwaj & Kundu, 2010; Gama e Silva et al., 2022).

The polymers used in electrospinning can be of natural or synthetic origin. Natural polymers, such as polysaccharides [e.g., cellulose, chitosan (CS), alginate] and proteins [e.g., silk fibroin, gelatin (GEL), collagen], usually present good biocompatibility and biodegradability, along with promoting cell adhesion due to specific sequences of "arginine-glycine-aspartic acid" amino acids in their structure (Bhardwaj & Kundu, 2010; Blanco-Fernandez et al., 2021). However, they can display mass variability, unfavorable mechanical properties, and the potential for denaturation. In contrast, synthetic polymers such as polycaprolactone (PCL), a polyester, are highly soluble in organic solvents and often exhibit more favorable mechanical properties when electrospun. These polymers can also demonstrate good biocompatibility, biodegradability, and enhanced adhesion to the skin (Bhardwaj & Kundu, 2010; Blanco-Fernandez et al., 2021; Darie-Niță et al., 2022; Deng et al., 2022). Combining natural and synthetic polymers may enhance mechanical properties, biocompatibility, and water absorption capacity (Li et al., 2022; Li et al., 2023). Table 1 summarizes some examples of polymers and their advantages.

There are electrospun nanofibrous products currently available on the market: Bioweb™, a membrane made from polyurethane and polytetrafluoroethylene, is used for the encapsulation of stents and other scaffolds (Zeus, 2023). Well microplates, produced by Nanofiber Solutions, feature both aligned and non-aligned fibers for cell culture applications (Nanofiber Solutions, 2023); NanoLayr products are designed for a variety of uses, including acoustic treatment, air filtration, mechanical property reinforcement, and active component delivery for skin

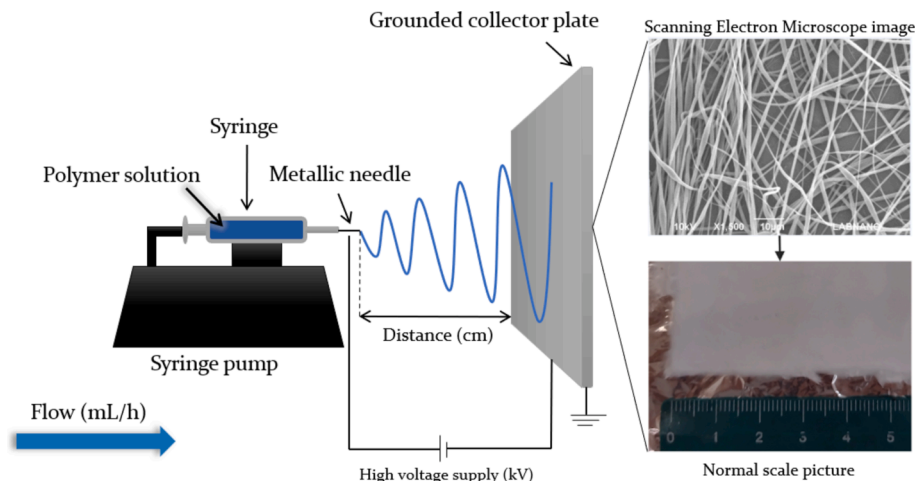


Fig. 1. Electrospinning equipment, parameters, and fiber/dressing images.

**Table 1**  
Examples of polymers used in electrospinning.

Polymer	Advantage	Published studies (2019–2023)*
Polycaprolactone (PCL)	Cost-effective; easy to process; slower degradation with fewer acidic by-products than other polyesters (Darie-Niță et al., 2022).	160
Polyvinyl alcohol (PVA)	Hydrophilic; maintains local humidity (Blanco-Fernandez et al., 2021).	126
Poly(ethylene glycol) (PEG)	Hydrophilic; maintains local humidity (Blanco-Fernandez et al., 2021).	14
Cellulose acetate (CA)	Hydrophilic; great absorption capacity; promotes cell adhesion (Hajjalayani et al., 2018).	26
Gum tragacanth (GT)	Accelerates regeneration by promoting cell signaling; calcium and magnesium ions facilitate cell migration and tissue regeneration (Hajjalayani et al., 2018).	2
Chitosan (CS)	Accelerates re-epithelialization and regeneration; antioxidant and anti-inflammatory activities; mucoadhesive; antibacterial activity due to positive charges on amino groups, which interact with negatively charged bacterial membranes; interferes in bacterial absorption of nutrients and metal ions from the environment (Aranaz et al., 2021; Croitoru et al., 2020; Simões et al., 2018).	141
Gelatin (GEL)	Hemostatic activity; low antigenicity; promotes cell adhesion (Blanco-Fernandez et al., 2021).	112

\* Studies searched in PubMed, excluding reviews, systematic reviews, book chapters, and other non-research documents. Keywords: “polymer name” AND electrospun AND wound healing (e.g., polycaprolactone AND electrospun AND wound healing).

care (NanoLayr, 2023); Neotherix offers membranes for tissue repair, treatment of fistulas, and antimicrobial action applications in dental or dermal contexts (Neotherix, 2023). Nano4Fibers provides nanofiber-based masks and membranes used in filtration, battery cells, and catalysis, among other applications (Nano4Fibers, 2023). These examples demonstrate the versatility of electrospun nanofibers, with applications spanning biomedical fields, filtration, battery cells, and acoustic treatments. Furthermore, a search conducted on the United States Patent and Trademark Office website revealed 2896 published patents for the

keywords “nanofiber AND healing” (August 2024).

Active components that promote tissue regeneration can also be of natural origin, exhibiting anti-inflammatory, antimicrobial, or antioxidant properties, among others. Natural products have been extensively studied in the last decades and have played a significant role in pharmacotherapy, accounting for over 40 % of all newly approved drugs (Atanasov et al., 2021; Newman & Cragg, 2012, 2020). This trend is also reflected in research on scaffolds for wound healing applications, where the number of studies focusing on nanofibers incorporating natural products has been increasing since 2009 (Fig. 2).

In addition, recently improved analytical tools, such as genome mining, engineering, and microbial culturing, have made it possible to overcome challenges in the screening, isolation, and characterization of natural products (Atanasov et al., 2021). Furthermore, compared to synthetic counterparts, the reduced toxicity and higher clinical trial success rates of natural products during drug development underscore their potential applications across various fields (Domingo-Fernández et al., 2024).

Natural products such as medicinal plants, essential oils, and honey are low-cost and easy to obtain. They offer good effectiveness, biocompatibility, and reduced adverse effects. When incorporated into nanofiber dressings, these products perform a synergistic role in wound relief and healing (Croitoru et al., 2020; Hajjalayani et al., 2018). Curcumin, for example, is a potent antioxidant that stimulates collagen synthesis and modulates the production of inflammatory cytokines (Hajjalayani et al., 2018). Terpenes, anthraquinones, saponins, flavonoids, and other secondary metabolites, as well as essential oils and plant extracts, may also exhibit antioxidant, anti-inflammatory, or antimicrobial activity (Hajjalayani et al., 2018; Simões et al., 2018). Honey is another active component with healing and antimicrobial properties, attributed to its high osmolarity and the presence of substances like hydrogen peroxide and defensin-1 (Simões et al., 2018).

The present study aimed to conduct a literature review on the production of nanofibers by electrospinning, embedding natural products such as plant extracts as active components for wound healing. Selected articles were compared based on the production methods, characterization, *in vitro* biological activity, and *in vivo* preclinical studies of the nanofibrous scaffolds.

## 2. Methodology

The work is a systematic review without meta-analysis, conducted in accordance with the PRISMA checklist (2020). The study was registered on the Systematic Review Facility (SyRF) platform (Bahor et al., 2021). The methodology followed the guidelines outlined in the PRISMA guide for systematic review without meta-analysis (Campbell et al., 2020).

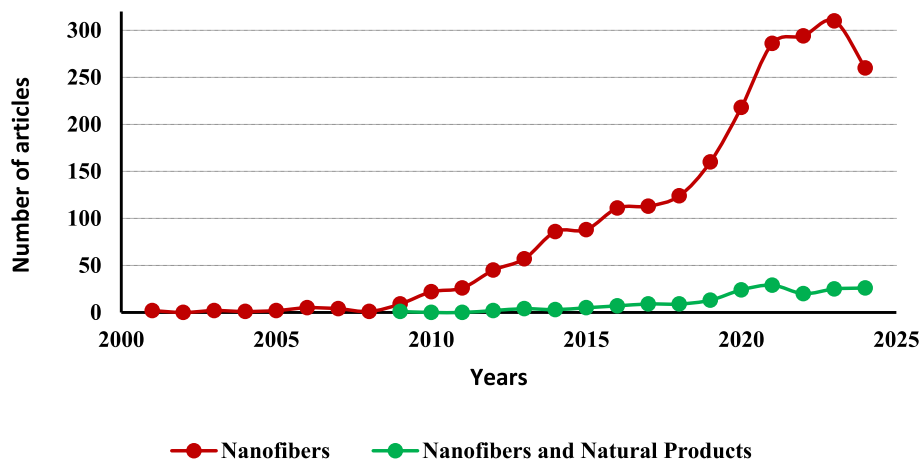


**Fig. 2.** Number of articles in the field of wound healing related to nanofibers and natural products. A search for the keywords “nanofibers AND wound healing” yielded 1952 articles, while “nanofibers AND wound healing AND natural products” returned 153 articles. Search conducted in August 2024.

SyRF (Bahor et al., 2021). <https://syrf.org.uk.ID:aa372b81-2fce-477a-a32d-4495c1622e25gSs3qs4vekejLUSVwWiuJQ==>.

### 2.1. Focused question

The main question answered by this work is: “Are nanofibers containing natural products effective in wound healing?”.

### 2.2. Search strategy

This systematic review covers the period from January 2011 to April 2024. The search was conducted using the PubMed and Web of Science databases with the following keywords: “nanofibers,” “nanofibers AND wound healing,” “nanofibers AND natural products,” “nanofibers AND wound healing AND natural products,” “nanofibers AND wound healing AND natural products AND *in vivo*.”

### 2.3. Inclusion criteria

Studies were included based on the following criteria: i) use of nanofibers as carriers for active components, with reported fiber diameter; ii) active substances of natural origin; iii) performance of *in vivo* tests or assays; iv) nanofibers containing natural active components for wound healing; v) *in vivo* evaluations of nanofibers containing natural products.

### 2.4. Exclusion criteria

The exclusion criteria were defined as follows: duplicate articles (present in both databases), review articles, patents, book chapters, abstracts, and studies that did not involve nanofibers, did not conduct *in vivo* tests, or did not use natural products as active components.

### 2.5. Study selection and screening process

Titles and abstracts of potentially relevant articles were initially screened to identify studies meeting the inclusion criteria. Full texts were obtained for articles deemed eligible after abstract screening. If the title and abstract did not provide sufficient information to determine eligibility, the full text was reviewed. The inclusion criteria were then applied to select relevant full-text articles, focusing on their materials, methods, and results. Three authors/reviewers conducted this screening process independently, and any questions or disagreements were resolved through group discussion. The remaining disagreements were resolved by a fourth reviewer.

### 2.6. Quality assessments

Quality assessments were conducted using the ARRIVE guidelines checklist (Kilkenny et al., 2010). A checklist comprising 24 items was developed based on these guidelines, and each criterion was graded as either “0” (not reported or not performed) or “1” (reported or performed). A final score was reported for each paper.

## 3. Results

A total of 110,088 results were retrieved using the “nanofibers” keyword: 4334 with “nanofibers AND wound healing,” 3222 with “nanofibers AND natural products,” 264 with “nanofibers AND wound healing AND natural products,” and 70 with “nanofibers AND wound healing AND natural products AND *in vivo*” (Table 2). The number of results from both databases was approximately equal at the end of the search.

The results retrieved using the “nanofibers AND wound healing AND natural products and *in vivo*” keywords were selected for further analysis and subjected to the inclusion and exclusion criteria (Fig. 3). Of the

**Table 2**

Number of articles found and keywords used.

Keywords	PubMed	Web of Science	Total
Nanofibers	25,716	84,372	110,088
Nanofibers AND wound healing	1837	2497	4334
Nanofibers AND natural products	789	2433	3222
Nanofibers AND wound healing AND natural products	143	121	264
Nanofibers AND wound healing AND natural products AND <i>in vivo</i>	42	28	70

70 results, 14 were excluded as review articles and four due to duplication, leaving 52 potential articles. Subsequently, four were excluded for not using nanofibers, 17 for not presenting active components of natural origin, and four for not reporting the fiber diameter. Additionally, one article was excluded due to restricted access. In total, 26 articles met the inclusion criteria and were selected.

Table 3 presents the assessment of the quality checklist results. Most studies had a clear title aligned with the paper’s content, except for three (Charernsriwilaiwat et al., 2013; García-Salinas et al., 2020; Mirhaj et al., 2024). In the abstract section, only eight papers provided background information on the active components, polymers, and techniques used. Only one study failed to clearly state its objectives (Kharat et al., 2021). Seventeen of the 26 studies reported electrospinning conditions, which are critical for reproducibility. All 26 studies performed morphological characterization of the electrospun fibers, but four did not include any other physicochemical characterization (Alberti et al., 2020; García-Salinas et al., 2020; Ke et al., 2021; Yao et al., 2019) using methods such as FTIR, XRD, DSC, or TGA. One study did not achieve an average fiber diameter of less than 1000 nm (Sharaf et al., 2021). Five studies conducted an *in vitro* scratch wound assay (Goher et al., 2024; Islam et al., 2022; Mirhaj et al., 2024; Nejaddehbashi et al., 2023; Nemati et al., 2021), and three did not perform any biocompatibility assay, such as the MTT (García-Salinas et al., 2020; Gupta et al., 2021; Terezaki et al., 2022). The performance of *in vivo* healing assays was an inclusion criterion, and thus, all studies scored 1 in this category. However, nine studies did not include an ethical statement or indicate adherence to guidelines. Four studies did not report any statistical methods (Kalachaveedu et al., 2020; Nemati et al., 2021; Sarhan & Azzazy, 2017; Sharaf et al., 2021). Only seven studies mentioned limitations, such as sample size and animal species chosen (Akbarpour et al., 2024; Goher et al., 2024; Kalachaveedu et al., 2020; Nejaddehbashi et al., 2023; Sarhan & Azzazy, 2017; Sharaf et al., 2021; Tahami et al., 2022). The average score across all studies was 18.65 out of 24, with the lowest score being 12 (Nemati et al., 2021) and the highest 24 (Goher et al., 2024). Notably, 25 out of the 26 studies scored above 15 points.

## 4. Discussion

### 4.1. Nanofibers, components, and production

Table 4 presents all information regarding the composition of the nanofibers, the active components used, the preparation conditions, and the characterization.

#### 4.1.1. Nanofibers

PVA was the most used polymer to obtain nanofibers, employed by 12 out of all 26 articles, followed by CS (six out of 22), various types of cellulose (six out of 22), and PCL (five out of 22). Other polymers were also used, such as polyethylene oxide (PEO), poly-L-lactic acid (PLLA), polyurethane (PU), various types of gums, GEL, and collagen. Fig. 4 presents the polymers used in the papers selected.

The synthetic polymers include PVA, PCL, poly(methyl methacrylate) (PMMA), PEO, and PU, with PVA being the most frequently used. PVA is a water-soluble polymer known for its ability to absorb proteins

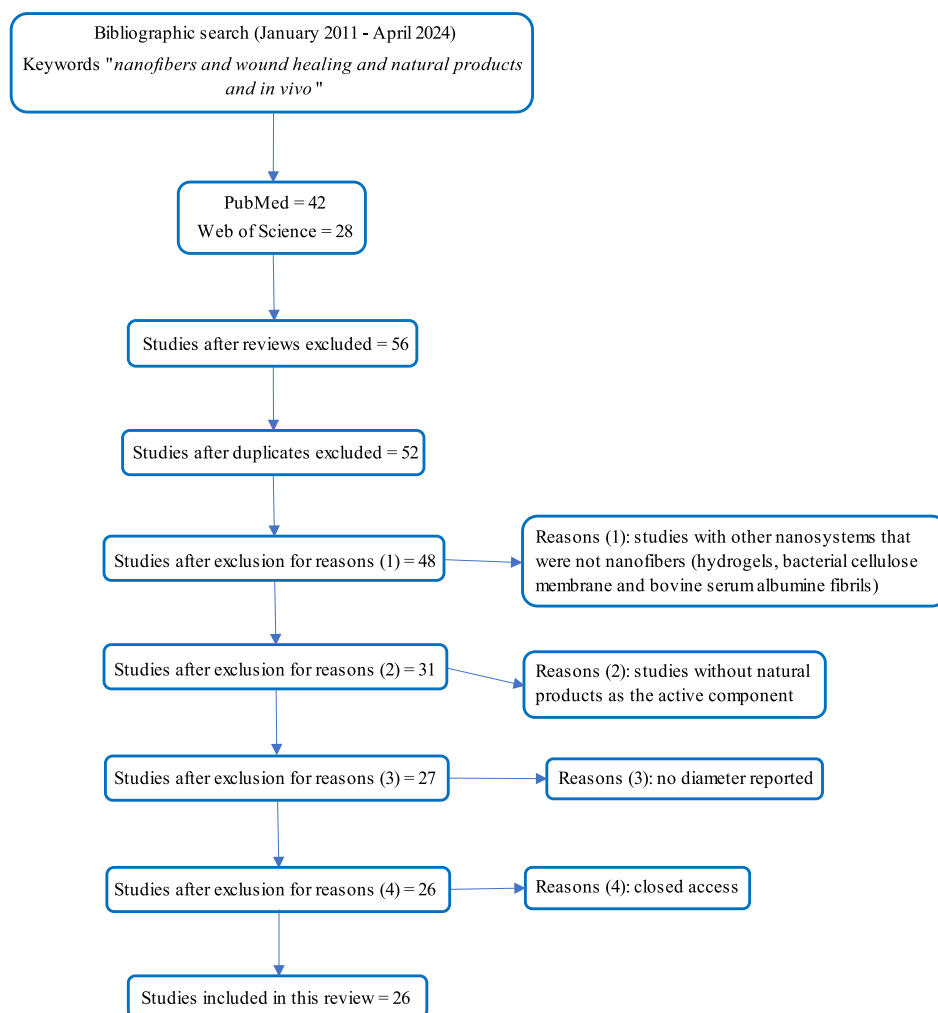


Fig. 3. Selection of the articles included in the literature review (Campbell et al., 2020).

and other substances, coupled with excellent biocompatibility, thermoplastic properties, and mechanical strength. It also offers the advantage of incorporating other polymers for electrospinning, making it a favorable choice for tissue regeneration (Gaaz et al., 2015). Additionally, PVA can be crosslinked using glutaraldehyde, enhancing its mechanical strength and stability (Deng et al., 2022). Many of the studies also incorporated CS, gums, collagen, GEL, or PCL with PVA, resulting in membranes with synergistic effects and improved chemical, mechanical, and thermal properties (Bhardwaj & Kundu, 2010).

The natural polymers include CS, cellulose, pectin, alginate, gums, GEL, collagen, hyaluronic acid, and PLA, with CS being the most frequently used. This preference is likely due to its ability to accelerate tissue regeneration and its well-established antimicrobial activity, which supports wound healing (Croitoru et al., 2020; Simões et al., 2018). Furthermore, CS-coated nanostructures promote cellular absorption, as the positive charge of CS binds to negatively charged lipids on the cell membrane of skin cells, promoting adhesion and increasing the permeation of compounds (Deng et al., 2022). This strategy was adopted by Sharaf et al. (2021). All the studies included CS in combination with PCL, PEO, PVA, or CA, leading to the development of electrospun membranes with novel properties (Bhardwaj & Kundu, 2010).

Only five papers used natural polymers alone (dos Santos et al., 2021; Farahani et al., 2020; Ke et al., 2021; Mirhaj et al., 2024; Sharaf et al., 2021), while three papers used only synthetic polymers (Alberti et al., 2020; Fahimirad et al., 2023; García-Salinas et al., 2020). Other

studies employed a combination of synthetic and natural polymers, which may enhance control over thermal, mechanical, and chemical properties, as well as stability and performance as a physical barrier at the wound site, and support cell adhesion during tissue regeneration (Bhardwaj & Kundu, 2010).

The effect of natural products on nanofibrous scaffolds varies. Studies that used PVA alone or in polymer blends observed either an increase (Akbarpour et al., 2024; Alberti et al., 2020; Charernsriwilaiwat et al., 2013; Fahimirad et al., 2023; Kalachaveedu et al., 2020; Salami et al., 2021; Sarhan & Azzazy, 2017; Tahami et al., 2022) or a decrease in fiber diameter and diameter distribution (Gupta et al., 2021; Islam et al., 2022; Sarhan & Azzazy, 2017). The influence on mechanical properties has also been reported, showing either an increase (Akbarpour et al., 2024; Kalachaveedu et al., 2020; Nemati et al., 2021), a decrease (Salami et al., 2021), or no effect/significant change (Charernsriwilaiwat et al., 2013; Fahimirad et al., 2023).

#### 4.1.2. Active components

Most papers used plant extracts (69 %) from leaves, flowers, or seeds incorporated into the polymer solution for electrospinning. Some (8 %) used isolated biosynthetic substances such as thymol and eugenol, while other studies used active bee-related components (15 %), including honey, propolis, and bee venom. Only two papers (8 %) used soy protein isolate. Fig. 5 summarizes the types of additives used.

In the last decades, extracts from plant products have gained significant attention due to their healing potential. Between 1993 and

**Table 3**  
Assessment of quality checklist.

Reference	(.Albertiet al., 2020)	(.Almasianet al., 2020)	(.Charensriwilaiwatet al., 2013)	(.dosSantoset al., 2021)	(.Eskandarimaet al., 2020)	(.Farahaniet al., 2020)	(.García – Salinaset al., 2020)	(.Guptaet al., 2021)	(.Kalachaveeduet al., 2020)	(.Keet al., 2021)	(.Kharafet al., 2021)	(.Nematiet al., 2021)	(.Salamiet al., 2021)	(.Sarhan&Azzazy, 2017)	(.Sharafet al., 2021)	(.Yaoet al., 2019)	(.Yousefiet al., 2017)	(.Terezakiet al., 2022)	(.Tahamiet al., 2022)	(.Islamet al., 2022)	(.Nejaddehbashiet al., 2023)	(.Fahimiradet al., 2023)	(.Goheret al., 2024)	(.Iraniet al., 2024)	(.Akbarpouret al., 2024)	(.Mirhajet al., 2024)
Title	1	1	0	1	1	1	0	1	1	1	1	1	1	1	1	1	1	1	1	1	1	1	1	1	1	0
Abstract	1	0	0	0	0	0	0	0	0	1	1	0	0	0	0	1	1	1	1	0	0	0	1	0	1	0
<b>Introduction</b>																										
Contextualization	1	1	1	1	1	1	1	1	1	1	1	1	1	1	1	1	1	1	1	1	1	1	0	1	1	
Objective	1	1	1	1	1	1	1	1	1	1	0	1	1	1	1	1	1	1	1	1	1	1	1	1	1	
<b>Methods</b>																										
Electrospinning conditions (voltage, distance, needle gauge, flow rate, collector type)	0	0	1	1	0	1	0	0	1	0	1	0	1	1	1	1	1	1	1	1	0	1	0	1	1	
Morphological characterization (SEM)	1	1	1	1	1	1	1	1	1	1	1	1	1	1	1	1	1	1	1	1	1	1	1	1	1	
Physicochemical characterization	0	1	1	1	1	1	0	1	1	0	1	1	1	1	1	0	1	1	1	1	1	1	1	1	1	
Nanometric size (<1000 nm)	1	1	1	1	1	1	1	1	1	1	1	1	1	1	0	1	1	1	1	1	1	1	1	1	1	
Ethics statement	1	0	1	0	1	1	1	0	0	0	1	0	1	0	0	1	1	1	1	1	1	1	0	1	1	
Study design	1	1	1	1	1	1	1	1	1	0	1	0	1	1	1	0	0	1	1	1	1	1	0	0	1	
<i>In vitro</i> healing study	0	0	0	0	0	0	0	0	0	0	0	1	0	0	0	0	0	0	0	1	1	0	0	0	1	
<i>In vitro</i> biocompatibility study	1	1	1	1	1	1	0	0	1	1	1	1	1	1	1	1	1	0	1	1	1	1	1	1	1	
<i>In vitro</i> antimicrobial study	0	1	1	0	1	1	0	1	0	0	1	1	0	1	0	0	1	0	0	1	1	1	1	1	1	
<i>In vivo</i> healing study	1	1	1	1	1	1	1	1	1	1	1	1	1	1	1	1	1	1	1	1	1	1	1	1	1	
Sample size	1	1	1	1	1	1	1	1	1	1	1	0	1	1	1	0	0	1	1	1	1	1	1	1	0	
Animal species	1	1	1	1	1	1	1	1	1	1	1	0	1	0	1	1	1	1	1	1	1	1	0	0	1	
Animal housing	1	1	0	0	0	1	1	0	1	1	0	1	0	1	0	1	0	1	1	0	1	1	1	0	1	
Animal gender	1	1	1	0	1	1	1	1	1	0	1	0	1	1	1	1	1	1	1	1	1	1	1	1	1	
Allocation to experimental groups	1	1	1	1	1	1	1	1	1	0	1	0	1	1	1	0	0	1	1	1	1	1	0	1	0	
Statistics	1	1	1	1	1	1	1	1	0	1	1	0	1	0	0	1	1	1	1	1	1	1	1	1	1	
<b>Results and Discussion</b>																										
Interpretation	1	1	1	1	1	1	1	1	1	1	1	1	1	1	1	1	1	1	1	1	1	1	1	1	1	
Limitations	0	0	0	0	0	0	0	0	1	0	0	0	0	1	1	0	0	0	1	0	1	0	1	0	0	
Conclusion	1	1	1	1	1	0	1	1	1	1	1	1	1	1	1	1	1	1	1	1	1	1	1	1	1	
Funding	1	1	1	1	1	1	1	1	1	1	0	1	1	1	0	0	1	1	0	1	1	1	1	1	1	
<b>Score</b>	<b>20</b>	<b>19</b>	<b>19</b>	<b>17</b>	<b>19</b>	<b>20</b>	<b>16</b>	<b>18</b>	<b>18</b>	<b>15</b>	<b>21</b>	<b>12</b>	<b>20</b>	<b>18</b>	<b>17</b>	<b>15</b>	<b>18</b>	<b>20</b>	<b>21</b>	<b>22</b>	<b>22</b>	<b>20</b>	<b>24</b>	<b>15</b>	<b>20</b>	<b>19</b>

**Table 4**  
Composition, physicochemical, and morphological characterization of nanofiber systems.

Reference	Composition	Electrospinning conditions	Characterization	Active components	Diameter
Alberti et al. (2020)	PVA 89–98 kDa 15 % (w/v) + propolis nanoparticles (1.7 mg/mL) (T7)	Flow rate: 0.02 mL/min, 20 kV, 12 cm, rotating collector roller at 200 rpm, 25 °C, 75 % humidity. No needle gauge.	SEM; no other methods.	Propolis extract (EtOH:H <sub>2</sub> O/70:30) encapsulated in nanoparticles (1.7 mg/mL of electrospinning solution).	325 ± 7 nm
Almasian et al. (2020)	PU/CMC (80:20 w/w) + 15 % <i>Malva sylvestris</i> dried flower extract	Flow rate: 0.6 mL/h, 16 kV, 12 cm, ambient temperature; no humidity, needle gauge, or collector type.	Swelling ratio, <i>in vitro</i> release, water vapor transmission rate, FTIR, mechanical properties, thickness, field-emission SEM; no EE or DL.	<i>Malva sylvestris</i> dried flower extract (EtOH:H <sub>2</sub> O/80:20)	386.5 nm
Charernsriwilaiwat et al. (2013)	2 % w/w CS-EDTA (2:1) + PVA 10 % w/v, 30:70 ratio + <i>Garcinia mangostana</i> dried hull extract	20 Gauge (0.9 mm) needle, 15 kV, 20 cm, 0.25 mL/h flow rate; rotating collector, room temperature; no humidity.	Viscosity, conductivity, surface tension of solution, SEM, FTIR, DSC, mechanical properties, swelling ratio, antioxidant activity, <i>in vitro</i> release, stability for six months.	<i>Garcinia mangostana</i> dried hull extract (70 % acetone) with 3 % alpha-mangosteen (w/w) to polymer.	251.3 ± 47.98 nm
dos Santos et al. (2021)	Cellulose acetate + CA- annatto ( <i>Bixa orellana</i> ) alcoholic seed extract (final polymer concentration: 12 % w/v)	0.3 mm diameter needle, 12 kV, 10 cm, rotation at 200 rpm, flow rate: 0.8 mL/h, room temperature; no humidity.	Thin layer chromatography (254 nm); NMR H1, FTIR, SEM, DSC, TGA; no release, EE or DL.	Annatto ( <i>Bixa orellana</i> ) alcoholic seed extract (20 ml + 5 g of polymer powder before electrospinning); final extract concentration: 0.1 % w/w.	269 ± 101 nm
Eskandarinia et al. (2020)	10 % w/w PU + 0.5 % w/w HA-DTA + 1 % ethanolic propolis extract (w/w to PU-HA).	21G needle; 20 cm, 18 kV, flow rate: 0.5 mL/h, 25 °C; no humidity; no collector.	FTIR, TGA, SEM, mechanical properties, contact angle, swelling ratio, <i>in vitro</i> release; no EE or DL.	1 % ethanolic propolis extract (EEP; 25 g in 250 mL of ethanol)	510 ± 45 nm
Farahani et al. (2020)	14 % w/v cellulose acetate/GEL (50:50) + ZM-nanoemulsion (soaking method: 1 cm <sup>2</sup> of nanofiber in 1 mL of ZM-nanoemulsion).	20G needle, flow rate: 1.19 mL/h, 15 kV, 14 cm, static collector, 30 % humidity, 25 °C.	SEM, mechanical properties, micro ATR-FTIR, <i>in vitro</i> release.	<i>Zataria multiflora</i> nanoemulsion (3 % essential oil v/v).	621 ± 98 nm
García-Salinas et al. (2020)	PCL + thymol (20 % w/w of PCL mass).	12,13 kV, 18 cm, flow rate: 1.0 mL/h, static collector; no temperature or humidity reported; no needle gauge.	SEM, <i>in vitro</i> release, mechanical properties, porosity.	Thymol (20 % w/w referred to as PCL mass).	299 ± 71 nm
Gupta et al. (2021)	10 % w/v PVA + 1 % w/v acacia gum solution (5:1 mix ratio) + EG-BCD (0.2 g in 6 mL polymer solution).	23 kV, 18 cm, flow rate: 0.5 mL/h; no needle gauge, temperature or humidity, no collector.	Field emission SEM, FTIR, TGA, XRD, AF-microscopy, swelling ratio, <i>in vitro</i> drug release.	Eugenol + beta-cyclodextrin powder (EG-BCD): 0.2 g in 6 mL of polymer solution.	171 ± 17 nm
Kalachaveedu et al. (2020)	1 % wt guar gum: 10 % wt PVA (3:7) + 20 % (of polymer wt) of <i>Acalypha indica</i> : <i>Aristolochia bracteolata</i> : <i>Thespesia populnea</i> : <i>Lawsonia inermis</i> ethanol extract (4:4:1:1); thermal crosslinking (5 % wt citric acid) at 40 °C for 48 h.	21G needle, flow rate: 0.5 mL/h, 20 kV, 18 cm, static collector; no temperature or humidity	FTIR, SEM, AFM, TGA, DSC, contact angle, swelling ratio, mechanical properties, protein adsorption study; no release, no EE or DL.	20 % (of polymer wt) of <i>Acalypha indica</i> (aerial parts): <i>Aristolochia bracteolata</i> (aerial parts): <i>Thespesia populnea</i> (bark): <i>Lawsonia inermis</i> (leaves) ethanol extract (4:4:1:1).	62–194 nm
Ke et al. (2021)	10 % PLLA w/w + SPI solution (mix ratio 8:2).	12 kV, 11 cm, flow rate: 1.2 mL/h; no needle gauge, collector type, temperature, or humidity.	SEM, DDPH assay; no other methods, release, EE, or DL.	Soy protein isolate 2 % w/w solution.	262 ± 64 nm for SPNF-100 and 157 ± 54 nm for SPNF-80
Kharat et al. (2021)	2 % CS solution (w/v):3% PEO solution (w/v) (70:30) + 2 % <i>Calendula officinalis</i> extract; crosslinking with glutaraldehyde.	18G needle, 18–20 kV, flow rate: 0.1–0.3 mL/h, rotating collector roller at 400 rpm, 13 cm, 24 °C and 20–30 % humidity.	SEM, FTIR, viscosity, conductivity, mechanical properties, swelling ratio and mass loss, contact angle, <i>in vitro</i> release; no EE or DL.	<i>Calendula officinalis</i> dried flower extract.	235.7 ± 94.74 nm
Nemati et al. (2021)	PVA (10 % wt solution)/BC (10 % wt solution)/g-C <sub>3</sub> N <sub>4</sub> -nettles- <i>Trachyspermum</i> (2 mL:200mL:120 mL); crosslinking with glutaraldehyde.	22G needle, 15 kV, flow rate: 0.25 mL/h, 15 cm; no humidity, temperature, or collector type.	SEM, FTIR, XRD, mechanical properties, swelling ratio, biodegradability test; no release, EE, or DL.	g-C <sub>3</sub> N <sub>4</sub> -nettles- <i>Trachyspermum</i> nanocomposite (dried nettles and 98 % <i>Carum copticum</i> ethanol extract).	430 nm
Salami et al. (2021)	PCL (12 % wt) + PVA-COL (10 % wt each) + <i>Momordica charantia</i> extract (10 % wt); crosslinking with glutaraldehyde.	10 cm, 20 kV, flow rate: 1 mL/min; rotating drum collector; no humidity, temperature, rpm.	SEM, contact angle, mechanical properties, swelling ratio, water vapor permeability, microbial penetration test; no release, EE, or DL.	<i>Momordica charantia</i> dried pulp water extract (10 % wt).	430 ± 54 nm
Sarhan & Azzazy (2017)	Honey:PVA:CS (30:7:3.5) + Bee venom (0.01 %) or propolis (10 %).	22G needle, 27 kV, 15 cm (13 cm for bacteriophage), flow rate: 0.5 mL/h, static collector; no temperature or humidity.	SEM, FTIR; no release, EE, or DL.	Bee venom (0.01 %; dry powder), propolis (10 %; 20 % aqueous ethanol extract), or bacteriophage solution (10 %).	HPCS-Pr: 737 nm ± 260 nm; HPCS-BV: 459 ± 140 nm; HPCS-BV-Bac: ~600 nm

(continued on next page)

Table 4 (continued)

Reference	Composition	Electrospinning conditions	Characterization	Active components	Diameter
Sharaf et al. (2021)	CA (15 % w/v) + CS-propolis nanoparticles; deacetylation with NaOH.	27G needle, 25 kV, flow rate: 1 mL/h, 20 cm, room temperature, and <50 % relative humidity.	SEM, FTIR, DSC, <i>in vitro</i> release, water contact angle.	CS-propolis nanoparticles (propolis 10 % w/v in 70 % ethanol for extraction; 10 mg of extract in nanoparticle solution).	1105 nm ± 345 nm
Yao et al. (2019)	2 % w-w CS solution (first layer) and GEL (9:1 pork:fish COL, 17 % wt sol) + PVA (10 % wt solution) (9:1, second layer) + <i>Lithospermi radix</i> extract; crosslinking layers with glutaraldehyde.	10 cm, 20 kV, flow rate: 0.1 mL/h, static collector (first layer); no needle gauge, temperature, or humidity.	SEM, <i>in vitro</i> release; no EE or DL.	<i>Lithospermi radix</i> (root) extract (75 % methanol; final concentration on nanofibers = 1.25 mg-mL).	182.86 ± 48.67 nm (without LR extract)
Yousefi et al. (2017)	3 % wt CS solution + PEO 4 % wt solution (90:10) + LI extract (2 % of polymer weight).	18G needle, flow rate: 1.5 mL/h, 5–25 kV, static collector, 10–20 cm, room temperature; no humidity.	SEM, mechanical properties, FTIR, swelling ratio, weight loss, porosity; no release, EE, or DL.	<i>Lawsonia inermis</i> dried leaves extract (ethanol 10 % v/v; final concentration = 2 % of polymer weight).	64 ± 8 nm
Terezaki et al. (2022)	ULV:PEO:GEL (2:1:1 or 1:1:2).	23G needle, 25 kV, 25 cm, flow rate: 1 mL/h for ULV: PEO solution, and 0.5–2 mL/h for GEL solution, rotating drum collector (400 rpm), 22 °C, 62 % humidity.	SEM, FTIR, TGA. No release, EE, or DL.	Ulvian solution at 4 % w/v (ULV; extracted from <i>Ulva rigida</i> ).	330 ± 97 nm for ULV:PEO:GEL (2:1:1); 331 ± 99 nm for ULV: PEO:GEL (1:1:2)
Tahami et al. (2022)	8 % PVA w/v solution + sodium alginate 2 % w/v solution (80:20) + <i>Calendula officinalis</i> extract (5, 10 and 15 %); crosslinking with glutaraldehyde and freeze-thawing.	18G needle, 15 cm, static collector, 15 kV, flow rate: 0.5 mL/h, no humidity or temperature.	SEM, FTIR, GEL fraction analysis, water vapor transmission rate, swelling ratio, <i>in vitro</i> release. No EE or DL.	<i>Calendula officinalis</i> extract at 10.7 % w/v (final concentrations on nanofibers are 5, 10, and 15 %).	220–360 nm
Islam et al. (2022)	10 % PVA (w/w) solution + 3 % CS (w/w) 0.5 M HCl solution + 0.5 % neomycin sulfate + 10 % (w/w) <i>Malva sylvestris</i> extract.	0.83 mm internal needle diameter, 15–20 kV, 10–20 cm, flow rate: 0.4–0.6 mL/h, room temperature. No humidity.	SEM, FTIR, swelling ratio, mechanical properties, <i>in vitro</i> release, porosity.	<i>Malva sylvestris</i> dried flower extract (EtOH:H <sub>2</sub> O/80:20).	194–401 nm
Nejaddehbashy et al. (2023)	15 % wt PCL solution + silver sulfadiazine (SSD) 3 mg/mL (first layer) and PCL 15 % wt solution + 1 % wt COL solution (70:30) (second layer); immersion in grape seed extract solution (2 % wt).	20 kV, 18 cm, flow rate: 0.5 mL/h, collector at 125 rpm (first layer); 17 kV, 16 cm, flow rate: 0.5 mL/h, collector at 125 rpm (second layer).	Field emission SEM, TGA, EDX, <i>in vitro</i> release.	Grape seed extract solution (2 % wt).	121.23 nm for PCL + SSD and 126.30 nm for PCL + COL
Fahimirad et al. (2023)	12 % wt PCL solution (first layer) + 10 % wt PVA solution and <i>Quercus infectoria</i> extract (4x MIC w/v%) and copper nanoparticles (6 × MIC w/v%).	22 kV, flow rate: 1 mL/h, 14 cm, rotating drum at 400 rpm. No needle gauge, temperature, or humidity.	Field emission SEM, FTIR, mechanical properties, swelling ratio, water vapor transmission rate, <i>in vitro</i> degradation and release, antioxidant activity. No EE or DL.	<i>Quercus infectoria</i> gall extract (QLG; 80 % methanol).	124.18 nm (PCL/PVA/QLG) and 152.81 nm (PCL/PVA/QLG/CuNPs)
Goher et al. (2024)	10 % PMMA (w/v) and 2 % CA (w/v) solutions (60:40) + PEO 1.5 % (w/v) + 0.01–0.02 % w/v extract.	20 kV, flow rate: 1 mL/h, drum collector at 600 rpm, spinneret width of 15 mm, distance of 12 cm, room temperature, humidity ~55 %.	SEM, ATR-FTIR, XRD.	<i>Tamarindus indica</i> extract (0.01, 0.015, and 0.02 % w/v).	300 ± 100 nm
Irani et al. (2024)	10 % PCL (w/v) + 3 % CS solution (w/v) + 3 % w/v extract; crosslink with glutaraldehyde.	20 kV, collector at 900 rpm. 15 cm, flow rate: 0.3 mL/h, 60 % relative humidity, room temperature.	SEM, FTIR, TGA, swelling ratio, weight loss.	<i>Dracaena cinnabari</i> ethyl acetate extract (3 % w/w).	270 ± 75 nm
Akbarpour et al. (2024)	12 % PVA solution + 2 % alginate solution + <i>Malva sylvestris</i> extract (7:2:1).	12 kV, 18G needle, flow rate: 0.4 mL/h, 12 cm, 25 °C. Crosslink with glutaraldehyde. No humidity.	Field emission SEM, FTIR, mechanical properties, water contact angle, water uptake, water vapor transmission rate, weight loss.	<i>Malva sylvestris</i> extract (10 %).	144 ± 30 nm
Mirhaj et al. (2024)	10 % wt cellulose solution (top layer); 10 % wt pectin solution + 10 % wt soy protein isolate solution (1:3) and 3 % wt extract.	1.23 mm inner diameter needle, 15 kV, 8 cm, flow rate: 1 mL/h (top layer); 0.6 mm inner diameter needle, 20 kV, 15 cm, flow rate: 1 mL/h (top layer).	Field emission SEM, FTIR, swelling ratio, mechanical properties, water vapor transmission rate, degradation, and soy protein isolate release.	<i>Punica granatum</i> peel extract (3 %) and soy protein isolate (75 % SPI solution).	60.65 ± 22.67 nm

**Key:** AFM: atomic force microscopy; ATR: attenuated total reflection; Bac: bacteriophage; BC: bacterial cellulose; BV: bee venom; CA: cellulose acetate; CMC: carboxymethyl cellulose; COL: collagen; CS: chitosan; DL: drug loading capacity; DSC: differential scanning calorimetry; DTA: dodecyl trimethylammonium; EE: encapsulation efficiency; EtOH: ethanol; FTIR: Fourier transform infrared spectroscopy; GEL: gelatin; HA: hyaluronic acid; NMR: nuclear magnetic resonance; NR: not reported; PCL: polycaprolactone; PEO: polyethylene oxide; PLLA: poly-L-lactic acid; PU: polyurethane; PVA: polyvinyl alcohol; SEM: scanning electron microscopy; TEM: transmission electron microscopy; TGA: thermogravimetric analysis; XRD: X-ray diffraction.



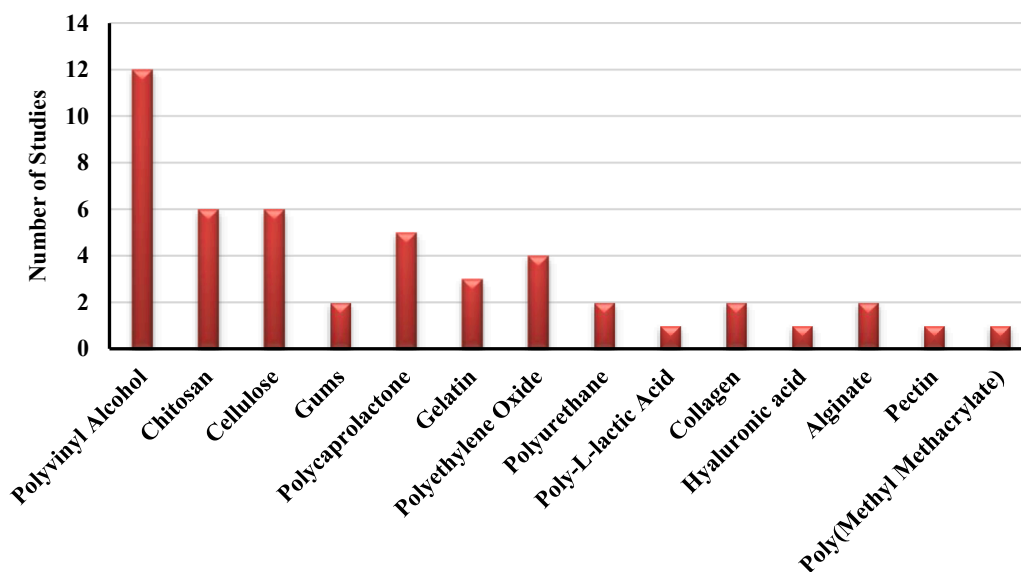


Fig. 4. Polymers used in the studies.

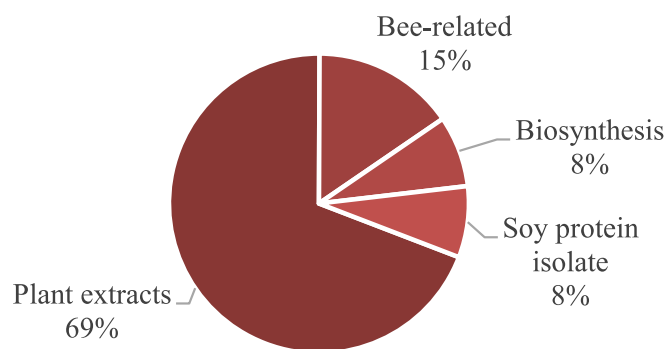


Fig. 5. Different active components used in the studies.

2013, nearly 450 plant species were investigated for their healing and antimicrobial properties, either *in vitro* or *in vivo*, for use in skin wound treatment (Ghosh & Gaba, 2013). Plant extracts can possess anti-inflammatory and antimicrobial activity, in addition to promoting tissue regeneration through the various substances present in their composition, such as terpenes, phenolic compounds (e.g., flavonoids), alkaloids, and others. These components can contribute to one or more phases of wound healing (Ghosh & Gaba, 2013; Pereira & Bártolo, 2016; Selvakumar et al., 2018). Furthermore, the ease and low cost of obtaining these extracts may explain their widespread use. One common method involves macerating vegetable matter, using various solvents (Selvakumar et al., 2018), followed by evaporation and lyophilization, which is less labor-intensive and expensive than the isolation and purification of specific metabolites.

Honey has gained significant attention in wound healing, particularly following the rise of bacterial resistance to antibiotics. Its anti-inflammatory and antioxidant properties make it a promising agent for wound management. Honey inhibits biofilm formation due to its high osmolarity, resulting from the large amount of sugar and low water content (Deng et al., 2022; Simões et al., 2018), and the presence of antimicrobial substances such as hydrogen peroxide and the defensin-1 peptide (Simões et al., 2018). Honey also promotes angiogenesis, facilitates debridement, activates the immune system, and stimulates the overall healing process (Scepankova et al., 2021). However, its use carries risks for individuals allergic to bee venom or those with diabetics (Deng et al., 2022; Simões et al., 2018). Similarly, propolis also has

antioxidant, anti-inflammatory, antibacterial, and antifungal activities due to the diverse range of substances in its composition (Banskota et al., 2001).

Isolated secondary metabolites can be the primary constituents responsible for the therapeutic effects of a natural product extract, particularly those derived from essential oils (Simões et al., 2018). Their use allows precise control over the concentration of active components in a formulation, enhancing the therapeutic effect compared to extracts or essential oils. However, the isolation process requires multiple extraction and purification steps, or the purchase of the substances as raw materials, which increases the associated costs.

The secondary metabolites used in isolation and the biochemical markers found in the extracts include alpha-mangosteen (xanthone) (Charemsriwilaiwat et al., 2013), bixin (carotenoid) (dos Santos et al., 2021), eugenol (phenylpropanoid) (Gupta et al., 2021), thymol (terpene) (García-Salinas et al., 2020), malvidin (polyphenol) (Almasian et al., 2020; Islam et al., 2022), faradiol myristate (triterpene) (Kharat et al., 2021; Tahami et al., 2022), lawsone (naphthoquinone) (Kalachaveedu et al., 2020; Yousefi et al., 2017), shikonin (naphthoquinone) (Yao et al., 2019), catechin (polyphenol) (Nejaddehbashi et al., 2023), and ulvan (polysaccharide) (Terezaki et al., 2022). Table 5 presents the molecular structure of the compounds and their biological activities.

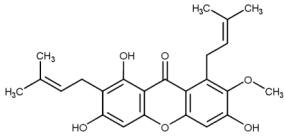
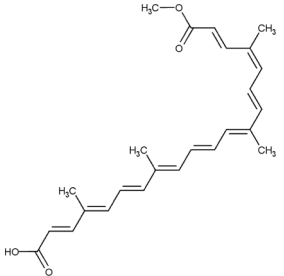
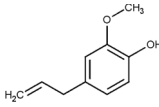
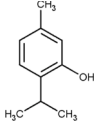
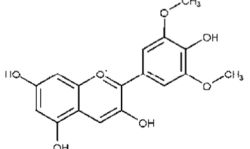
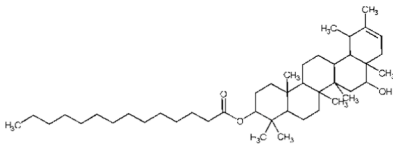
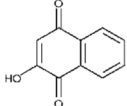
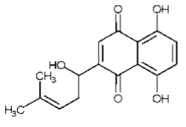
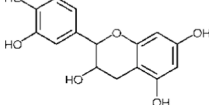
#### 4.1.3. Preparation method

Most articles produced a single-layer electrospun membrane embedding natural products, a process known as 2D electrospinning (Keirouz et al., 2020). Recently, the process of obtaining 3D (double-layered) membranes has emerged, offering additional advantages compared to 2D membranes (one layer), such as remarkable similarity to the extracellular matrix, porosity, enhanced water uptake capacity, and a larger surface area for cell migration and adhesion (Keirouz et al., 2020).

Yao et al. (2019) produced a double-layered membrane, where the first layer consisted of a lyophilized and crosslinked CS matrix with good water uptake ability. The second layer was a GEL-PVA electrospun membrane containing *Lithospermi radix* extract, designed for wound healing.

Nejaddehbashi et al. (2023) also obtained a double-layered membrane. The first consisted of PCL with silver sulfadiazine, an antimicrobial agent, while the second layer was PCL with collagen. The membrane was immersed in a grape seed extract solution to assess its

**Table 5**  
Molecules in plant extracts or used as isolated active compounds.

Reference	Substance	Biological activity	Chemical structure
Charensriwilaiwat et al. (2013)	Alpha-mangosteen	Antioxidant, antibacterial, accelerated wound healing.	
dos Santos et al. (2021)	Bixin	Antioxidant, antibacterial, and anti-inflammatory.	
Gupta et al. (2021)	Eugenol	Antifungal and wound healing.	
García-Salinas et al. (2020)	Thymol	Antibacterial and anti-inflammatory.	
Almasian et al. (2020); Gasparetto et al. (2012); Islam et al. (2022)	Malvidin	Antioxidant and anti-inflammatory.	
Fronza et al. (2009); Kharat et al. (2021); Tahami et al. (2022)	Faradiol myristate	Fibroblast migration and proliferation.	
Kalachaveedu et al. (2020); Nayak et al. (2007); Yousefi et al. (2017)	Lawsone	Antibacterial, antioxidant, and wound healing.	
Yao et al. (2019)	Shikonin	Cell differentiation and wound healing.	
Nejaddehbashi et al. (2023)	Catechin	Antioxidant.	

(continued on next page)

Table 5 (continued)

Reference	Substance	Biological activity	Chemical structure
Terezaki et al. (2022)	Ulvan	Antioxidant, antiviral, anticoagulant, antihyperlipidemic, and antitumor.	

healing potential and antimicrobial effects.

Similarly, Fahimirad et al. (2023) produced a double-layered membrane, with the first layer made of PCL and the second layer composed of PVA, copper nanoparticles, and *Quercus infectoria* extract. Mirhaj et al. (2024) also developed a double-layered membrane, where the first layer was made of cellulose microfibrils and the second layer consisted of pectin, soy protein isolate, and *Punica granatum* peel extract. Both studies report the creation of a supportive and protective layer, over which another layer is electrospun to embed the active components.

#### 4.1.4. Morphological and physicochemical characterization

Several techniques were used to characterize the nanofibers, including SEM, infrared spectroscopy, TGA, XRD, mechanical property evaluations, active component release studies, and stability assessments. Fig. 6 summarizes the number of characterization techniques used in the reviewed articles. A total of 65.4 % of the papers employed more than five techniques or assays to characterize the nanofibers, while 15.4 % used only one or two techniques, of which one corresponds to SEM.

All articles used at least SEM for the characterization of the nanofibers. The average diameter range reported across the studies varied from 60 nm to 1100 nm. A total of 57.7 % of the papers exclusively employed FTIR spectroscopy (including the ATR mode), while 3.8 % employed only the water contact angle method. Additionally, 19.2 % of the papers used both techniques. Another 3.8 % utilized energy-dispersive X-ray spectroscopy technique, making up 84.6 % of the studies that characterized the chemical composition of the membranes. Regarding thermal behavior and stability, 7.6 % of the papers performed DSC, 19.2 % used only TGA, and 7.6 % used both techniques, resulting in 34.4 % of the studies assessing the thermal behavior and stability of the nanofibers.

Only 11.5 % of the papers performed XRD to verify the crystallinity

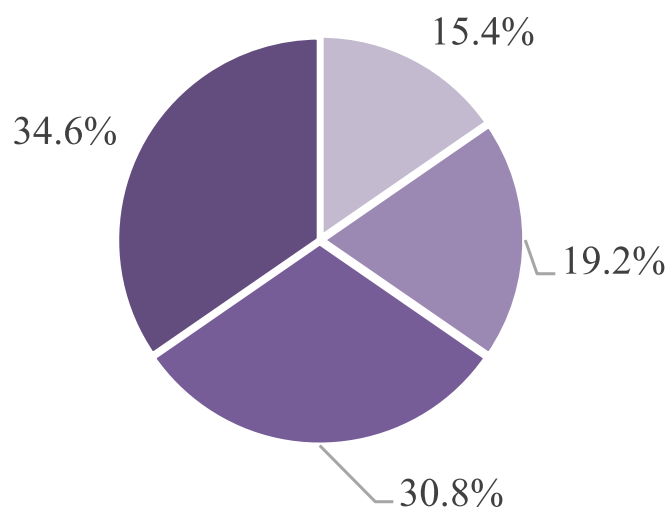


Fig. 6. Number of characterization techniques used in the studies.

of the membranes. In contrast, 53.8 % carried out *in vitro* release assays, an important parameter to determine the kinetics and mechanism of active component release. These assays aim to prevent sudden release of large amounts of the active ingredient, which could lead to toxicity, or slow release that may diminish the therapeutic effect (Ambekar & Kandasubramanian, 2019). Additionally, 53.8 % of the studies evaluated the mechanical properties of the membranes, an important parameter for biomedical applications, as dressings must endure the tension and forces associated with tissue growth, as well as physical and daily activities (Bhardwaj & Kundu, 2010).

The same active components can influence scaffold properties differently based on both solution composition and electrospinning parameters, as mentioned before. For instance, studies using *Malva sylvestris* extracts demonstrated either an increase or decrease in water uptake and average fiber diameter, as well as enhanced mechanical properties for PVA and PU scaffolds (Akbarpour et al., 2024; Almasian et al., 2020; Islam et al., 2022). *Calendula officinalis* also resulted in different effects when embedded into nanofibers. Tahami et al. (2022) reported increased fiber diameter and reduced water uptake in PVA/Alg scaffolds, whereas Kharat et al. (2021) found the opposite effect in CS/PEO nanofibers. These differences highlight the importance of employing multiple characterization techniques to thoroughly evaluate the impact of natural products on nanofibrous scaffolds.

#### 4.2. In vitro assays

Table 6 presents information about the cell viability and antimicrobial activity in *in vitro* tests.

Most studies conducted *in vitro* cell viability tests using the 3-(4,5-dimethylthiazolyl)-2,5-diphenyltetrazolium bromide (MTT) assay, with only one study using the Neutral Red Uptake Assay (Alberti et al., 2020). Other assays employed include the CAM cytotoxicity test (dos Santos et al., 2021; Mirhaj et al., 2024), scratch wound assay (Goher et al., 2024; Islam et al., 2022; Mirhaj et al., 2024; Nejaddehbashi et al., 2023; Nemati et al., 2021), lactate dehydrogenase assay (Irani et al., 2024), and hemolysis assay (Salami et al., 2021). Fibroblasts were the most commonly used cell line in 19 of the 26 articles, followed by cells from the human umbilical cord matrix, mesenchymal stem cells, and keratinocytes. Notably, only three of the 26 articles did not report any cell viability tests. Fig. 7 provides a summary of these findings.

The MTT reduction test is widely used and relies on the assumption that viable cells can convert the soluble tetrazolium salt [3-(4,5-dimethylthiazol-2-yl)-2,5-diphenyltetrazolium bromide] (MTT) into an insoluble formazan precipitate. This occurs when tetrazolium salts accept electrons from oxidized substrates or enzymes like NADH and NADPH (Supino, 1995). The resulting crystals must be solubilized to enable spectrophotometric reading. The method's practicality, affordability, and availability of commercial kits (Riss et al., 2004) likely account for its widespread use in the reviewed studies. Moreover, the frequent use of fibroblasts in *in vitro* assays is due to their crucial role in wound healing. Fibroblasts migrate to the wound to form granulation

Table 6

In vitro assays.

Reference	Viability	Antibacterial	Results
Alberti et al. (2020)	Murine NIH/3T3 fibroblast for neutral red uptake assay (540 nm).	NR	NR
Almasian et al. (2020)	Human umbilical cord matrix (hUCM) for MTT assay (540 nm); cell morphology and adhesion to scaffold assays.	<i>S. aureus</i> , ATCC 6538 and <i>E. coli</i> ATCC 8739 (CFU count).	Antibacterial percentage against <i>S. aureus</i> was 69.83 % (MIC 2.4 mg/mL) and, for <i>E. coli</i> , 70.66 % (MIC 2.11 mg/mL)
Charernsrilwaiwat et al. (2013)	Human foreskin fibroblast (NHF) for MTT assay (550 nm).	<i>S. aureus</i> ATCC 6538P and <i>E. coli</i> ATCC 10536 (optical density at 550 nm).	MIC and MBC of 0.5 mg/mL for <i>S. aureus</i> and <i>E. coli</i> .
dos Santos et al. (2021)	HET-CAM cytotoxicity assay; mouse fibroblast WT C57BL6 for MTT assay (595 nm); cell morphology and adhesion to scaffold.	NR	NR
Eskandarinia et al. (2020)	L929 fibroblasts for MTT (575 nm); cell morphology and adhesion to scaffold.	<i>S. aureus</i> ATCC 25923 and <i>E. coli</i> ATCC 25922 (disc diffusion on agar).	Antibacterial effect of $2.36 \pm 0.33$ for <i>E. coli</i> and of $1.94 \pm 0.12$ for <i>S. aureus</i> (no diameter for inhibition zone).
Farahani et al. (2020)	L929 fibroblasts for MTT assay (570 nm); cell morphology and adhesion to scaffold.	<i>S. aureus</i> ATCC 33591 and <i>E. coli</i> ATCC 25922 (disc diffusion on agar).	Higher antibacterial activity than blank NFs (no numerical data, just visual).
García-Salinas et al. (2020)	NR	NR	NR
Gupta et al. (2021)	NR	<i>Candida albicans</i> (CA) ATCCMYA 2876 and <i>Candida glabrata</i> (CG) ATCC 90030 for XIT assay (biofilm inhibition and eradication on agar) and counting (dilution and incubation on agar); fungi morphology and adhesion to scaffold.	30 mg samples inhibited growth >75 %, 10 mg samples inhibition was 75 % for CA and 90 % for CG, and eradication was 60 % for CA and 80 % for CG.
Kalachaveedu et al. (2020)	Gingival mesenchymal stem cells for MTT assay (530 nm).	NR	NR
Ke et al. (2021)	L929 fibroblasts for MTT assay (no nanometer or $\lambda$ ); cell morphology and adhesion to scaffold.	NR	NR
Kharat et al. (2021)	Human skin fibroblasts (NR)	<i>S. aureus</i> ATCC 33591, <i>E. coli</i> ATCC 35218	The inhibition zone for <i>E. coli</i> and <i>S. aureus</i> was

Table 6 (continued)

Reference	Viability	Antibacterial	Results
	cell line) for MTT assay (570 nm).	(agar well diffusion and viable cell count).	$20.9 \pm 1.1$ (mm) and $22.0 \pm 0.4$ (mm), respectively; CS/PEO/CO nanofibers presented a 96.9 % reduction in <i>S. aureus</i> and a 94.8 % reduction in <i>E. coli</i> colony counts, and CS/PEO nanofibers showed a 14.9 % reduction in <i>S. aureus</i> and a 30.0 % reduction in <i>E. coli</i> colony count.
Nemati et al. (2021)	NIH 3 T3 fibroblasts for MTT (570 nm) and scratch wound assays.	<i>E. coli</i> and <i>S. aureus</i> (dilution and incubation on agar); NR ATCC.	Wound closure of 70 % in scratch wound assay for the PVA/BC/g-C3N4-nettles-trachyspermum NF (24 h). MIC of the nanofibers was <0.01 mg/mL for <i>E. coli</i> and <2 mg/mL for <i>S. aureus</i> .
Salami et al. (2021)	Hemolysis assay; L929 fibroblasts for MTT (570 nm).	NR	NR
Sarhan & Azzazy (2017)	Human fibroblast cells (ATCC 2522) for MTT assay (595 nm).	<i>E. coli</i> , <i>S. aureus</i> , MRSA and MDR <i>P. aeruginosa</i> (viable cell count).	No activity against <i>P. aeruginosa</i> , ~6 log reduction for <i>S. aureus</i> and 3–5 log reduction for MRSA; HPSC-BV completely inhibited <i>E. coli</i> but HPSC-Pr had no significant effect; HPSC-BV-Bac inhibited <i>P. aeruginosa</i> .
Sharaf et al. (2021)	HFB4 fibroblast cells for MTT assay (560 nm).	NR	NR
Yao et al. (2019)	L929 mouse fibroblasts for MTT assay (no nanometer or $\lambda$ ); cell morphology and adhesion to scaffold.	NR	NR
Yousefi et al. (2017)	Normal human foreskin fibroblast for MTT assay (570 nm); cell morphology and adhesion to scaffold.	<i>S. aureus</i> and <i>E. coli</i> (disc diffusion on agar) (lysogeny broth medium); (NR ATCC).	Inhibition zone of 25 mm for <i>E. coli</i> and of 18 mm for <i>S. aureus</i> .
Terezaki et al. (2022)	NR	NR	NR
Tahami et al. (2022)	L929 fibroblasts for MTT assay (570 nm).	NR	NR
Islam et al. (2022)	Human umbilical cord matrix (hUCM) for MTT assay; Balb/3t3 fibroblasts for	<i>S. aureus</i> ATCC 6538 and <i>E. coli</i> ATCC 8739 (colony counting).	Antibacterial effect of 69.85 % against <i>S. aureus</i> and 70.69 % against <i>E. coli</i> .

(continued on next page)

Table 6 (continued)

Reference	Viability	Antibacterial	Results
	scratch wound assay.		Cells treated with NF + extract moved faster than control or neomycin nanofibers.
Nejaddehbashi et al. (2023)	Human dermal fibroblasts for MTT (570 nm) and scratch wound assay; cell morphology and adhesion to scaffold.	<i>S. aureus</i> ST ATCC 29213 and <i>P. aeruginosa</i> OS ATCC 27853.	Inhibition zone of 8 mm for <i>S. aureus</i> and 11 mm for <i>P. aeruginosa</i> for double-layered nanofibers, against 0 mm for nanofibers without silver sulfadiazine.
Fahimirad et al. (2023)	Human dermal fibroblasts for MTT assay.	MRSA (optical density); NR ATCC.	PCL/PVA/CuNPs 6xMIC, PCL/PVA/QLG 4xMIC, and PCL/PVA/QLG/CuNPs inhibited bacterial growth.
Goher et al. (2024)	Human normal skin fibroblast (HBF4) for MTT (570 nm) and scratch wound assays.	<i>Salmonella paratyphi</i> , <i>E. coli</i> , <i>S. aureus</i> , <i>Bacillus cereus</i> , <i>C. glabrata</i> , and <i>C. albicans</i> (colony counting and optical density at 600 nm). No ATCC was reported.	0.02 % <i>T. indica</i> nanofibers showed biofilm inhibition >60 % against all pathogens except <i>Candida</i> spp.
Irani et al. (2024)	Human skin fibroblasts (NR cell line) for MTT assay (570 nm) and LDH assay (490 nm).	<i>S. aureus</i> , <i>Bacillus subtilis</i> , <i>E. coli</i> , <i>P. aeruginosa</i> (disc diffusion on agar). No ATCC reported.	NF + 3 % extract showed similar inhibition zones for all pathogens compared to positive control (gentamycin).
Akbarpour et al. (2024)	L929 fibroblasts for MTT assay (540 nm).	<i>S. aureus</i> and <i>E. coli</i> (optical density at 600 nm). No ATCC was reported.	NF + 10 % extract showed antibacterial activity of 41.39 ± 3.99 % and 31.48 ± 3.28 % against <i>S. aureus</i> and <i>E. coli</i> , compared to 5.66 ± 1.83 % and 7.24 ± 2.03 % for blank fibers, respectively.
Mirhaj et al. (2024)	HaCaT keratinocytes for MTT (570 nm) and scratch wound assays; CAM cytotoxicity assay; cell morphology and adhesion to scaffold.	<i>S. aureus</i> and <i>E. coli</i> (colony counting). No ATCC was reported.	NF + 3 % extract showed >90 % antibacterial activity against <i>S. aureus</i> , compared to ~80 % for cellulose/pectin/soy protein isolate NF, and ~50 % for Cel/Pec NF, and showed ~90 % activity against <i>E. coli</i> , compared to ~80 % for Cel/Pec/SPI NF and ~50 % for Cel/Pec NF.

**Key:** Bac: bacteriophage; BC: bacterial cellulose; BV: bee venom; CO: *Calendula officinalis*; COL: collagen; CS: chitosan; CuNPs: copper nanoparticles; *E. coli*: *Escherichia coli*; ESBL: extended-spectrum beta-lactamase; HPCS: honey:PVA:CS;

KFG:M-PG:C: keratin:fibrin:gelatin:mupirocin-3-hydroxybutyric acid:gelatin:curcumin; LDH: lactate dehydrogenase; Li: *Lawsonia inermis*; MBC: minimal bactericidal concentration; MDR: multidrug-resistant; MIC: minimal inhibitory concentration; MRSA: methicillin-resistant *Staphylococcus aureus*; NF: nanofibers; NR: not reported; *P. aeruginosa*: *Pseudomonas aeruginosa*; PCL: polycaprolactone; PEO: polyethylene oxide; Pr: propolis; PVA: polyvinyl alcohol; QLG: *Quercus infectoria* extract; *S. aureus*: *Staphylococcus aureus*.

tissue, produce and secrete collagen, proteoglycans, and glycosaminoglycans, and ultimately contract the wound (Berthet et al., 2017; Han & Ceilley, 2017; Sorg & Sorg, 2023).

The studies also assessed the antimicrobial activity of the scaffolds produced. Most papers used *Staphylococcus aureus* and *Escherichia coli* strains (16 and 13 of all 26 articles, respectively), including methicillin-resistant *S. aureus* (MRSA) strains. Few studies evaluated *Pseudomonas aeruginosa* strains, with some even testing against multidrug-resistant *P. aeruginosa* (MDR). Additionally, two studies tested against *Candida* spp. However, 10 out of the 26 studies performed no antimicrobial testing. Fig. 8 provides a summary of these findings.

*Staphylococcus aureus* is the most commonly isolated pathogen in skin infections, ranging from mild to severe cases, including necrosis. Since it is part of the skin microbiota, wounds can easily lead to infection (Harris-Tryon & Grice, 2022; Hatlen & Miller, 2021; Yang et al., 2022). Gram-negative pathogens, particularly *E. coli*, stand out (Cardona & Wilson, 2015; Jabbour & Kanj, 2021). These factors account for the frequent use of these species in antimicrobial tests.

#### 4.3. In vivo assays

Table 7 presents information about the animal models and experimental groups used.

All the studies selected performed *in vivo* tests, a requirement for inclusion in the present review. Among them, 58 % used Wistar rats, with 13 employing male rats, one using female rats, and another not specifying the gender. Additionally, 11 % of the studies used Sprague-Dawley rats, with two employing male rats and one omitting gender details. Various mouse species were also used, totaling 23 % of the studies, including Swiss and SKH1 hairless mice. Two of these studies did not report the gender (Nemati et al., 2021; Sarhan & Azzazy, 2017). One study used rabbits for *in vivo* healing tests (Irani et al., 2024). Fig. 9 summarizes the data on the type of animals used in the *in vivo* studies.

Rat and mouse species are commonly used *in vivo* in the biomedical field, particularly to evaluate the efficacy or other parameters of active substances, emphasizing Sprague-Dawley and Wistar rats and Swiss mice, respectively (Zwierzyzna & Overington, 2017). However, we noted a predominance of Wistar rats over Sprague-Dawley rats. These findings contrast with data reported nearly 20 years ago by Dorsett-Martin (2004), who found that Sprague-Dawley rats (56.36 %) were more commonly used than Wistar rats (27.27 %) in skin wound healing research. Although mice might offer lower costs, the more frequent use of rats observed by Zwierzyzna and Overington (2017), Dorsett-Martin (2004), and in the current paper may be attributed to factors such as their larger size, ease of handling, predictable nature, and more extensive skin surface for wound studies (Dorsett-Martin, 2004; Grada et al., 2018).

The data on animal gender align qualitatively with the findings of Dorsett-Martin (2004), as most studies also used male rats. Possible explanations are that male mice cost less than females of the same weight or that female wounds heal more easily by contraction due to thinner skin, whereas male rats undergo epithelialization during the wound-healing process (Dorsett-Martin, 2004).

The articles reviewed employed various wound models in the *in vivo* studies. The majority (62 %) used normal wound models in healthy animals, such as excision or incision wounds. Other models included streptozotocin-induced diabetes wounds (15 %), burn wounds (15 %), and wounds infected with *S. aureus* (8 %). Fig. 10 summarizes the types

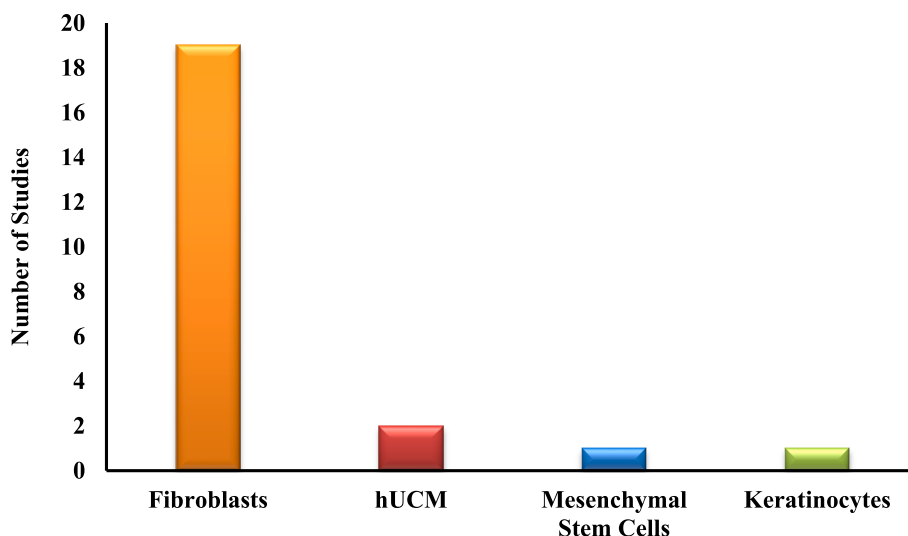


Fig. 7. Different cell lines were used for viability tests in the studies.

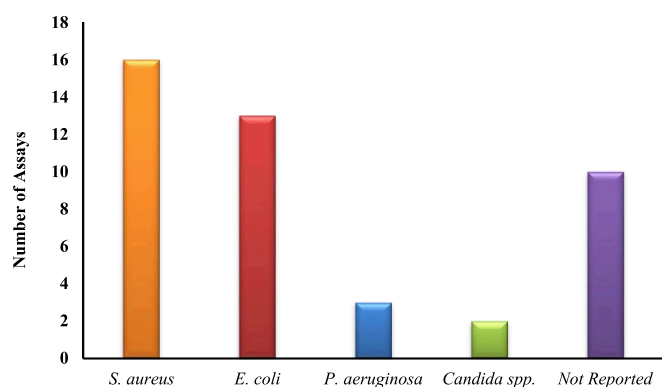


Fig. 8. The different species used for antimicrobial tests in the studies retrieved for the present review.

of wounds used in the animal models in these studies.

The use of excision wounds in healthy individuals allows for studying wound healing chronology (closure) and physiology (cell types and structures involved). On the other hand, burn wounds facilitate the evaluation of antimicrobial activity and the prevention of infections (Berthet et al., 2017). Both excision/incision and burn models represent acute wounds (Grada et al., 2018). Diabetic models provide insight into delayed healing or chronic wounds, as well as models with infection, which allow for direct evaluation of the antimicrobial ability of the formulation (Berthet et al., 2017; Grada et al., 2018). The predominance of the acute wound models highlights the focus on testing the wound-healing properties of membranes and natural components and evaluating the morphophysiological changes they induce in tissue, often compared to a standard treatment or control.

The data found in the current paper are also similar to those by Dorsett-Martin (2004), who observed that 76.36 % of studies used excision/incision wound models, 18.18 % employed prolonged wound models (such as diabetic and infected wounds), and 12.72 % used burn wounds (compared to 62 % excision/incision, 23 % prolonged, and 15 % burns in this research). Although there is a reduction in the number of models by excision/incision and an increase in models of prolonged wounds, it is worth noting that the current paper evaluated 26 articles, approximately half of the total assessed by those authors.

Only three of the 26 studies did not mention any percentage of wound closure or wound area (dos Santos et al., 2021; García-Salinas et al., 2020; Sharaf et al., 2021). Terezaki et al. (2022) used a scoring

system to assess skin parameters and evaluate the wound healing potential in a burn-wound model. They found the best scores (2/15 and 3/15) for ulvan-embedded PEO/GEL nanofibers after 26 days of treatment, whereas control and blank fiber groups scored between 7.5 and 10/15. Irani et al. (2024) observed the remaining area of a 1.50 × 1.50 cm wound in male rabbits and reported a complete wound closure for *D. cinnabari*-loaded nanofibers after 14 days of treatment, compared to a remaining area of 0.60 × 0.50 cm for blank scaffolds, 1.50 × 0.70 cm in the control group, and 0.50 × 0.30 cm in the sulfadiazine group.

Among the articles that evaluated excision/incision wounds for 21 days, Eskandarinia et al. (2020) reported a complete wound closure after treatment with PU/HA scaffolds embedding ethanolic propolis extract, compared to a remaining wound area of 6.11 % for blank nanofibers and ~20 % for the control group. Gupta et al. (2021) observed a complete wound closure for the positive control and eugenol-loaded nanofiber groups, compared to ~80 % for blank nanofiber and negative control groups. Tahami et al. (2022) detected a wound closure of 97.18 % using PVA/Alginate nanofibers embedding 10 % *Calendula officinalis* extract, compared to 93.06 % for blank nanofibers and 79.41 % for the control group.

In the group of papers that evaluated excision/incision wound models for a period of ~14 days, Nemati et al. (2021) reported a 95 % wound closure after treatment with nettle and *Trachyspermum* extract-loaded PVA/bacterial cellulose nanofibers, compared to ~80 % for blank fiber and ~60 % for control groups. Salami et al. (2021) found similar results for the treatment, blank, and control groups after treatment with *Momordica charantia* extract-loaded PCL/PVA/COL nanofibers. Fahimirad et al. (2023) achieved 100 % wound closure after treatment with PCL/PVA scaffolds embedding *Quercus infectoria* extract and copper nanoparticles, whereas other treatment groups achieved <75 % wound closure (uninfected animals) and <90 % (MRSA-infected animals). Control groups achieved less than 50 % wound closure in both cases. Mirhaji et al. (2024) achieved ~90 % wound closure for nanofibers embedding *Punica granatum* extract and soy protein isolate, compared to ~80 % for NF-soy protein isolate group, ~50 % for blank fiber, and ~40 % for control groups. Goher et al. (2024) reported >90 % wound closure for *Tamarindus indica* extract-loaded scaffolds and blank fibers, compared to 48.4 % for the control group.

For burn wounds treated within ~21 days, Farahani et al. (2020) obtained the highest healing rate, with a relative wound area of 11.2 % for animals treated with nanofibers embedding *Zataria multiflora* nano-emulsion, compared to 37.6 % for control and 36.9 % for blank fiber groups. Within 14 days of treatment, Akbarpour et al. (2024) achieved 93.94 % wound closure for *Malva sylvestris*-loaded PVA/alginate

Table 7

In vivo assays.

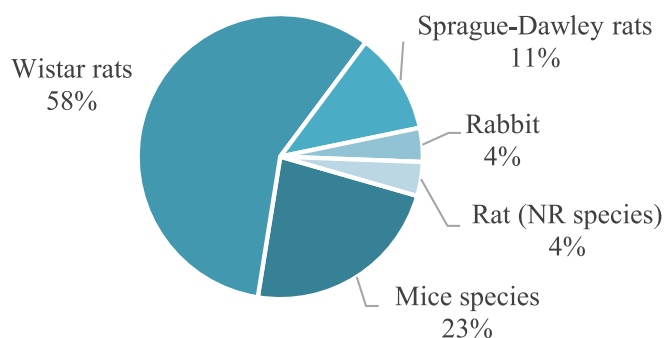
Reference	Animal Model	Study Model	Experimental Groups	Results
Alberti et al. (2020)	Male Swiss mice	Streptozotocin experimental diabetes + 0.8 cm diameter skin wound.	Four groups (n = 4 in each): propolis nanoparticles scaffold (T7), vehicle scaffold (blank nanoparticles), negative control (no treatment), and positive control (allantoin solution 2.5 mg/mL).	On day 7, the wound closure percentages were as follows: negative control (20.7 % ± 10.47), positive control (54.3 % ± 4.8), blank NF (54.3 % ± 4.8), T7 (68.8 % ± 12.9)
Almasian et al. (2020)	Male Wistar rats	Streptozotocin experimental diabetes + 1.5 cm diameter skin wound.	Three groups (n = 5 in each). Group A = extract containing nanofibers; Group B = PU/CMC; Group C = conventional gauze bandage; histological analysis.	On day 14, the wound closure percentages were as follows: gauze bandage (32.1 ± 0.2 %), PU/CMC (51.4 ± 0.4 %), PU/CMC/15 (95.05 ± 0.24 %).
Charernsriwilaiwat et al. (2013)	Male Wistar rats	0.8 cm <sup>2</sup> skin wound.	Four groups (n = 6): positive control (antibacterial gauze), negative control (gauze), and 0 % and 3 % alpha-mangosteen; histological analysis.	On day 10, CS-EDTA/PVA + 3 % alpha-mangosteen showed the highest and fastest wound closure (~100 %), similar to the positive control, compared to ~97 % for other groups.
dos Santos et al. (2021)	Wistar rats (NR gender)	(2x) 5 mm skin wound.	Two groups: Group A (n = 4): cellulose acetate/ <i>Anatto</i> nanofibers; Group B (n = 2): no treatment. Wound healing was assessed 15 and 60 days after treatment; histological analysis.	No wound closure %; no scarring and good biocompatibility during the 60 days.
Eskandarinia et al. (2020)	Female Wistar rats	11 mm diameter skin wound.	Three groups (n = 8 in each): no treatment, PU and PU-HA/EEP 1 %; histological analysis.	On day 21, 0 % of the remaining wound area for the PU-HA/EEP1% group, compared to 6.11 % ± 0.2 % of the PU group and ~20 % for the control group.
Farahani et al. (2020)	Male Wistar rats	2 cm <sup>2</sup> burn wound was created using a metal bar at 100 °C for 30 s.	Five groups (n = 7 in each): gauze, CA nanofibers (drug-free), CA/GEL nanofibers (drug-free), CA/ZM-nano and CA/gel/ZM-nano groups; histological analysis.	On day 22, the CA/gel/ZM-nano group showed a relative wound area of 11.2 ± 1.3 %, compared to 37.6 ± 2.8 % for control, 36.9 ± 2.5 % for CA-NF drug-free, and 24.4 ± 1.9 % for CA/ZM- NF.
García-Salinas et al. (2020)	Male SKH1 hairless mice	8 mm diameter skin wound + infection with <i>S. aureus</i> ATCC 25923.	Five groups (n = 6 in each): control, PCL, PCL-THY, THY alone, and chlorhexidine; histological analysis.	No wound closure evaluation; two log reductions in bacterial growth of <i>in vivo</i> samples for PCL-THY and chlorhexidine on day 3, moderate bacterial growth for both at the wound site on day 7.
Gupta et al. (2021)	Male albino Wistar rats	8 mm diameter skin wound.	Five groups (n = 5 in each): no treatment/-ctrl, neosporin/+ctrl, blank NF, 1 g of EG-NF, and 2 g of EG-NF; histological analysis.	On day 21, 100 % wound closure for + ctrl and 2 g EG-NF, 90 % for 1 g EG-NF, and ~80 % for blank NF and -ctrl.
Kalachaveedu et al. (2020)	Male Wistar rats	1.5 cm <sup>2</sup> skin wound.	Five groups (n = 6 in each): no treatment, cotton gauze, blank nanofiber mat, R120 nanofiber, R120 nanofiber + gingival mesenchymal stem cells; histological analysis.	On day 14, 97.83 ± 0.17 % wound closure for the R120 + GMS cells group, 96.82 ± 0.24 % for R120 group, 93.17 ± 0.34 % for blank nanofiber mat and 92.91 ± 0.33 % for cotton gauze group.
Ke et al. (2021)	12 New Zealand rabbits for hemostatic test; Sprague-Dawley rats (NR gender)	12 mm diameter skin wound.	Four groups (n = 16 total): gauze, Hydrocolloid Dressing (HCD), SPNF-100, and SPNF-80 groups; histological analysis.	On day 15, wound closure was >90 % for SPNF-80, similar to HCD; On day 6, the relative wound area was 55.40 ± 1.43 % for the gauze group, 30.28 ± 2.00 % for the HCD group, 34.76 ± 1.23 % for the SPNF-100 group and 26.19 ± 0.47 % for the SPNF-80 group.
Kharat et al. (2021)	Male Wistar rats	2 cm <sup>2</sup> skin wound.	Six groups (n = 4 in each): sterile gauze, CS/PEO nanofibers, CS/PEO/CO nanofibers; histological analysis.	On day 14, the CS/PEO/CO dressing wound closure index was 87.5 ± 1.8 %, 79.4 ± 1.5 % for CS/PEO, and ~65 % for control.
Nemati et al. (2021)	Mice (NR gender or species)	1 cm <sup>2</sup> skin wound.	Four groups (NR n): no treatment, dressing with phenytoin cream, PVA dressing, and PVA/BC/g-C3N4-nettles- <i>Trachyspermum</i> nanofibers; histological analysis.	On day 14, wound closure for PVA/BC/g-C3N4-nettles- <i>Trachyspermum</i> NF was 95 %, compared to ~70 % for phenytoin, ~60 % for control, and ~80 % for blank PVA-NF.
Salami et al. (2021)	Male Wistar rats	1 cm diameter skin wound.	Five groups (n = 6 each): no treatment, PCL-PVA-COL-MCext 0 %, 1 %, 5 % and 10 %; histological analysis.	On day 14, NFs + 10 % extract group showed 94.01 ± 8.12 % wound closure, compared to 55.54 % ± 5.32 % for control and ~80 % for blank NFs.
Sarhan & Azzazy (2017)	Male mice (NR species)	9 mm diameter skin wound.	Five groups (n = 3 in each): +Ctrl (Aquacel Ag), -Ctrl (cotton gauze), HPCS-BV, HPCS-Pr, and HPCS-Bac; histological analysis.	On day 12, ~100 % wound closure for all NF and Aquacel Ag groups, and ~80 % for cotton gauze group.
Sharaf et al. (2021)	Male <i>Mus musculus</i> mice	2 cm <sup>2</sup> burn wounds (no temperature or burn degree reported).	Four groups (n = 4 in each): free propolis (+Ctrl), blank NF, CA-CS-Pr nanofibers, cotton gauze (-Ctrl); histological analysis.	On day 21, the CA-CS-Pr groups presented decreased wound area, compared to other groups (no percentage).
Yao et al. (2019)	Male Sprague-Dawley rats	(6x) 15 mm <sup>2</sup> skin wound.	Six wound treatments (NR n): GF91 membrane, GF91L, GF100, CS scaffold, commercial wound dressing (Comfeel), and gauze control.	On day 14, the wound closure rates were 84.65 ± 6.5 % for GF91, 87.13 ± 2.68 % for GF91L, 80.13 ± 5.21 % for GF100, 79.5 ± 6.42 % for CS scaffold, 76.93 ± 6.5 % for Comfeel, and 74.26 ± 5.97 % for gauze control groups.
Yousefi et al. (2017)	Male Wistar rats	2 cm <sup>2</sup> skin wound.	Three groups (NR n): LI extract ointment, blank NF and 2 % LI extract NF.	On day 14, ~96 % wound closure for 2 % LI extract-NF, compared to ~90 % for blank NF and ~84 % for ointment.

(continued on next page)

Table 7 (continued)

Reference	Animal Model	Study Model	Experimental Groups	Results
Terezaki et al. (2022)	Male SKH-hr1 hairless mice	Second-degree burn wound.	Eight groups (n = 6 each): 1) ULV/PEO (2:1); 2) ULV/PEO (1:1); 3) GEL:PEO (2:1); 4) GEL/PEO (1:1); 5) ULV/PEO/GEL (2:1:0,5); 6) ULV/PEO/GEL (2:1:1); 7) ULV/PEO/GEL (1:1:2); 8) PEO nanofibrous patch; histological analysis.	On day 26, ULV/PEO/GEL (1:1:2) showed full wound closure and had the best burn wound healing score (2/15), with mild inflammation, followed by ULV/PEO/GEL (2:1:1) with a score of 3/15. Other groups obtained a higher score, ranging from 7.5/15 – 10/15.
Tahami et al. (2022)	Male Wistar rats	(5x) 1x1 cm <sup>2</sup> wound.	One group (n = 9), each wound treated accordingly: control (gauze); PVA/Salg; PVA/Salg/CA5%; PVA/Salg/CA10%; PVA/Salg/CA15%; histological analysis.	On day 21, 10 % extract-NF group showed 97.18 % wound closure, compared to 79.41 % for control and 93.06 % for blank (PVA/Salg) nanofibers. Other nanofibers showed less than 91 % wound closure.
Islam et al. (2022)	Male Wistar rats	Streptozotocin experimental diabetes + 1.5 cm diameter skin wound.	Three groups (n = 5 in each). Group A = extract containing nanofibers; Group B = PVA/CS/Neomycin sulfate nanofibers; Group C = Conventional gauze bandage; histological analysis.	On day 14, 96.08 % wound closure for NF + plant extract, 89.64 % for PVA/CS/Neomycin sulfate nanofibers, and 56.84 % for gauze group.
Nejaddehbashi et al. (2023)	Male Sprague-Dawley rats	Streptozotocin experimental diabetes (for diabetic group) + bilateral 100 mm <sup>2</sup> skin wound (on every rat).	Three groups (n = 9 in each): 1- Normal rats treated with double-layered NF with and without GSE; 2- Diabetic rats treated with double-layered NF with and without GSE; 3- gauze group (control); histological analysis.	On day 14: the wound closure was ~90 % for Normal/GSE + group, 85.81 % for Diabetic/GSE + group, 84.23 % for Normal/GSE- group, 75.7 % for Diabetic/GSE- group, and 43.93 % for gauze group.
Fahimirad et al. (2023)	Male Wistar rats	2x2 cm <sup>2</sup> wound; infection with MRSA for infected groups.	Twelve groups (n = 6 in each): PCL; PCL/PVA; PCL/PVA/QLG; PCL/PVA/CuNPs; PCL/PVA/QLG/CuNPs; Control (gauze). Each group had an infected and uninfected counterpart; histological analysis.	On day 15, PCL/PVA/QLG/CuNPs nanofibers showed ~100 % wound closure for uninfected and infected groups, compared to <75 % and <90 % wound closure for other treatments, respectively. Ctrl groups showed <50 % wound closure in both groups.
Goher et al. (2024)	Male Wistar rats	8 mm diameter wound.	Five groups (n = 4 each): Sterile gauze; NF without extract; NF + 0.01 % extract; NF + 0.015 % extract; NF + 0.02 % extract; histological analysis.	On day 14, the NF + 0.02 % extract group showed 97.7 % wound closure, similar to other groups, compared to 48.4 % in the control group.
Irani et al. (2024)	Male rabbits (NR species)	1.5 × 1.5 cm diameter wound.	Five groups (n = 15 total): gauze dressing (control); silver sulfadiazine; CS-PCL NFs; NF + 3 % extract; NF + 3 % ethyl acetate extract.	On day 14, the NF + 3 % ethyl acetate extract group showed complete wound closure, compared to the 0.20 × 0.05 cm wound area for NF + 3 % extract, 0.60 × 0.50 cm for blank NFs, 1.50 × 0.70 cm in the control and 0.50 × 0.30 cm wound area in the silver sulfadiazine group.
Akbarpour et al. (2024)	Male rats (NR species)	1.2 × 1.2 cm burn wound created using a stainless-steel shaft at 100 °C for 8 s.	Three groups (n = 12 in each): no treatment (control); blank PVA:alginate mats; PVA: alginate: <i>M. sylvestris</i> extract mats; histological analysis.	On day 21, NF + Eextract showed 93.94 ± 3.101 % wound closure, compared to 77.34 ± 2.63 % for blank mats and 59.51 ± 2.54 % for control group.
Mirhaj et al. (2024)	Male Wistar rats	1 cm <sup>2</sup> wound.	Four groups (NR n): untreated wound (control); cellulose/pectin NF; Cel/Pec/soy protein isolate NF; Cel/Pec/SPI/ <i>P. granatum</i> extract NF; histological analysis.	On day 12, NF + extract showed ~90 % wound closure, compared to ~80 % for Cel/Pec/SPI NF, ~50 % for Cel/Pec NF, and >40 % for the control group.

**Key:** Bac: bacteriophage; BC: bacterial cellulose; BV: bee venom; CA: cellulose acetate; Chit@Nep/Hon: chitosan:*Nepeta dschuparensis*:honey; CMC: carboxymethyl cellulose; CO: *Calendula officinalis*; COL: collagen; CS: chitosan; CuNPs: copper nanoparticles; EEP: ethanolic propolis extract; GEL: gelatin; GSE: grape seed extract; HA: hyaluronic acid; HPCS: honey:PVA:CS; KFG:M-PG:C: keratin:fibrin:gelatin:mupirocin-3-hydroxybutyric acid:gelatin:curcumin; Li: *Lawsonia inermis*; MRSA: methicillin-resistant *Staphylococcus aureus*; NR: not reported; NF: nanofibers; PCL: polycaprolactone; PEO: polyethylene oxide; Pr: propolis; PU: polyurethane; PVA: polyvinyl alcohol; QLG: *Quercus infectoria* extract; *S. aureus*: *Staphylococcus aureus*; SPNF: soy protein nanofibers; GT: tragacanth gum; THY: thymol; ZM: *Zataria multiflora*; ±Ctrl: positive/negative control.

Fig. 9. Different animal species used for *in vivo* tests in the studies.

nanofibers, compared to 77.34 % for blank scaffold and 59.51 % for control groups.

In the group of studies that used a diabetic wound model treated for ~14 days, Almasian et al. (2020) obtained 96.08 % wound closure using PVA/CS/neomycin sulfate nanofibers embedding *Malva sylvestris* extract, compared to 89.64 % and 56.84 % for the blank fiber and control groups, respectively. Islam et al. (2022) reported similar results, achieving 95.05 % wound closure for *M. sylvestris*-loaded nanofibers, compared to 54.4 % for blank fiber and 32.1 % for control groups.

Li et al. (2024) also produced scaffolds for diabetic wound models. They achieved over 99 % wound closure after 18 days of treatment with electrospun nanoyarn-constructed dressings embedding *Salvia miltiorrhiza* bunge-radix pueraria herb extract, compared to 90.0 % for blank scaffolds and 86.6 % for the control group. This result indicates the potential wound healing application of traditional Chinese plants and, furthermore, points to the use of novel nanoyarn-constructed scaffolds



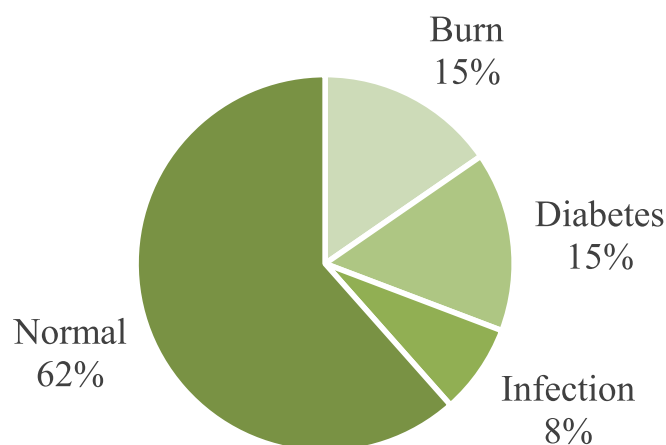


Fig. 10. Different wound models used for *in vivo* tests in the studies.

as dressings. Wang et al. (2024) also used different electrospinning approaches, obtaining radially-oriented nanofibrous scaffolds embedding the quinoline alkaloid berberine. After 18 days of treatment, berberine-loaded radially oriented nanofibers resulted in 100 % wound closure, compared to 85 % for the control group, 86 % for randomly oriented blank scaffolds, and 95 % for radially oriented blank scaffolds.

#### 4.3.1. Clinical studies

A search on the “clinicaltrials.gov” platform for “all studies” using the terms “scaffold” AND “wound heal” resulted in 79 studies using different delivery systems, whereas the search employing different combinations of the terms “nanofiber,” “electrospun,” “wound heal,” “wound heal delayed” AND “wound infection” only found two results. The study of the “EktoTherix™ tissue regeneration matrix” product (“wound heal” AND “electrospun”) for surgical excision wounds began in 2015, reaching its endpoint in 2017. It evaluated its safety and regenerative and healing capacity, as well as the cosmetic activity (scar) after the treatment, corresponding to one of the products based on nanofibers already mentioned. The randomized controlled trial “Comparing wound complication following TMA with the aid of electrospun fiber matrix” (“wound infection” AND “electrospun”) was estimated to start in November (2023) to compare infection rates and wound closure after transmetatarsal amputation (TMA) treated using electrospun fiber matrix.

Another search applying the combination of terms “wound healing” AND “nanofibers” found one result corresponding to a randomized multicenter controlled trial for rotator cuff repair using a nanofiber scaffold. The study began in 2020, enrolling patients over 55 years whose primary diagnosis is rotator cuff tear, aiming to evaluate whether there is a difference in post-operative healing, strength, and functional outcomes.

## 5. Limitations and future perspectives

Tissue regeneration is a natural phenomenon involving multiple stages and cell types. Interference by infections, exogen, and endogen factors in this process can result in hard-to-heal wounds. The search for better treatments for wound healing using natural products is remarkable in the literature due to biocompatibility and various substances with therapeutic effects in their composition.

Electrospun membranes embedding active components of natural origin emerge as a promising alternative treatment, as they present good biocompatibility and biodegradability and modulate the release of substances, promoting and accelerating wound healing.

In the current review, most studies produced single-layered membranes, whereas few studies used electrospinning to obtain double-layered membranes or a single membrane made of two polymers,

allowing different active components in each polymeric solution. Moreover, plant extracts were the main active component. *In vitro* tests mainly used fibroblasts for viability and healing assays. *Staphylococcus aureus* and *E. coli* are the main pathogens selected for evaluating antimicrobial activity. Most of the analyzed studies used acute wound models and used male Wistar rats for *in vivo* tests.

Our review detected that natural products can affect nanofibrous scaffolds differently, such as increasing or reducing fiber diameter, mechanical properties, and water uptake ability. Therefore, multiple characterization techniques are required to fully access the scaffold properties and evaluate its application as a dressing. Moreover, natural products can affect the healing process and accelerate wound closure compared to control and blank nanofibers groups, indicating the potential application for wound healing approaches.

Despite the potential observed, some challenges hinder the effective development of a final product. Plant extraction is a slow process that usually presents low yield, requiring significant amounts of plant material for increased production. Building an industrial facility for producing nanofibrous membranes also involves environmental control of rooms and laboratories, generating more expenses in addition to the high cost of industrial electrospinning devices. Clinical tests are another high-cost step involving trained professionals and the production of sufficient amounts of membranes embedding natural products for treating and monitoring patients for months or years.

#### Informed consent statement

Not applicable.

#### Ethics approval

Not applicable as no human or animals were involved in this study.

#### CRediT authorship contribution statement

**Breno de Almeida Bertassoni:** Writing – original draft, Investigation, Data curation. **Denise de Abreu Garófalo:** Writing – review & editing, Methodology. **Mariana Sato de Souza Bustamante Monteiro:** Writing – review & editing, Formal analysis. **Ralph Santos-Oliveira:** Writing – review & editing, Methodology. **Anne Caroline Candido Gomes:** Writing – review & editing, Methodology. **Anna Leticia Martinez Martinez Toledo:** Writing – review & editing, Formal analysis. **Marcos Lopes Dias:** Writing – review & editing, Formal analysis. **Naomi Kato Simas:** Writing – review & editing, Methodology. **Eduardo Ricci-Junior:** Writing – review & editing, Supervision, Methodology, Funding acquisition.

#### Funding

This paper was supported by the following institutions: Carlos Chagas Filho Foundation for Research Support from the State of Rio de Janeiro (*Fundação Carlos Chagas Filho de Amparo à Pesquisa do Estado do Rio de Janeiro*, FAPERJ) – *Cientista do Nosso Estado* (CNE) [Grant number: E-26/201.077/2021]; Support for *Stricto Sensu* Graduate Programs in the State of Rio de Janeiro [Grant number: E-26/210.136/2021]; *RedeNano Saúde* [Grant number: E-26/010.000981/2019]; and Conselho Nacional de Desenvolvimento Científico e Tecnológico (CNPq) - PQ-1D - Research Productivity Scholarship [Grant number: 309790/2023-9] awarded to Eduardo Ricci-Júnior.

#### Declaration of competing interest

The authors declare that they have no known competing financial interests or personal relationships that could have appeared to influence the work reported in this paper.

## References

- Akbarpour, A., Rahimnejad, M., Sadeghi-Aghbash, M., Feizi, F., 2024. Poly(vinyl alcohol)/Alginate nanofibrous mats containing Malva Sylvestris extract: synthesis, characterization, in vitro and in vivo assessments for burn wound applications. *Int. J. Pharm.* 654 (January). <https://doi.org/10.1016/j.ijpharm.2024.123928>.
- Alberti, T.B., Coelho, D.S., de Prá, M., Maraschin, M., Veleirinho, B., 2020. Electrospun PVA nanoscaffolds associated with propolis nanoparticles with wound healing activity. *J. Mater. Sci.* 55 (23), 9712–9727. <https://doi.org/10.1007/s10853-020-04502-z>.
- Almasian, A., Najafi, F., Eftekhari, M., Ardekani, M.R.S., Sharifzadeh, M., Khanavi, M., 2020. Polyurethane/carboxymethylcellulose nanofibers containing Malva sylvestris extract for healing diabetic wounds: preparation, characterization, in vitro and in vivo studies. *Mater. Sci. Eng. C* 114 (May 2019). <https://doi.org/10.1016/j.msec.2020.111039>.
- Ambekar, R.S., Kandasubramanian, B., 2019. Advancements in nanofibers for wound dressing: a review. *Eur. Polym. J.* 117 (April), 304–336. <https://doi.org/10.1016/j.eurpolymj.2019.05.020>.
- Aranaz, I., Alcántara, A.R., Civera, M.C., Arias, C., Eloora, B., Caballero, A.H., Acosta, N., 2021. Chitosan: an overview of its properties and applications. *Polymers* 13 (19). <https://doi.org/10.3390/polym13193256>.
- Atanasov, A.G., Zotchev, S.B., Dirsch, V.M., Orhan, I.E., Banach, M., Rollinger, J.M., Barreca, D., Weckwerth, W., Bauer, R., Bayer, E.A., Majeed, M., Bishayee, A., Bochkov, V., Bonn, G.K., Braidy, N., Bucar, F., Cifuentes, A., D'Onofrio, G., Bodkin, M., Supuran, C.T., 2021. Natural products in drug discovery: advances and opportunities. *Nat. Rev. Drug Discov.* 20 (3), 200–216. <https://doi.org/10.1038/s41573-020-00114-z>.
- Bahor, Z., Liao, J., Currie, G., Ayder, C., MacLeod, M., McCann, S.K., Bannach-Brown, A., Wever, K., Soliman, N., Wang, Q., Doran-Constant, L., Young, L., Sena, E.S., Sena, C., 2021. Development and uptake of an online systematic review platform: the early years of the CAMARADES systematic review facility (SyRF). *BMJ Open Sci.* 5 (1), 1–10. <https://doi.org/10.1136/bmjos-2020-100103>.
- Banskota, A.H., Tezuka, Y., Kadota, S., 2001. Recent progress in pharmacological research of propolis. *Phytother. Res.* 15 (7), 561–571. <https://doi.org/10.1002/ptr.1029>.
- Berthet, M., Gauthier, Y., Lacroix, C., Verrier, B., Monge, C., 2017. Nanoparticle-based dressing: the future of wound treatment? *Trends Biotechnol.* 35 (8), 770–784. <https://doi.org/10.1016/j.tibtech.2017.05.005>.
- Bhardwaj, N., Kundu, S.C., 2010. Electrospinning: a fascinating fiber fabrication technique. *Biotechnol. Adv.* 28 (3), 325–347. <https://doi.org/10.1016/j.biotechadv.2010.01.004>.
- Blanco-Fernandez, B., Castaño, O., Mateos-Timoneda, M.A., Engel, E., Pérez-Amodio, S., 2021. Nanotechnology approaches in chronic wound healing. *Adv. Wound Care* 10 (5), 234–256. <https://doi.org/10.1089/wound.2019.1094>.
- Campbell, M., McKenzie, J.E., Sowden, A., Katikireddi, S.V., Brennan, S.E., Ellis, S., Hartmann-Boyce, J., Ryan, R., Shepperd, S., Thomas, J., Welch, V., Thomson, H., 2020. Synthesis without meta-analysis (SWiM) in systematic reviews: reporting guideline. *The BMJ* 368, 1–6. <https://doi.org/10.1136/bmj.l6890>.
- Cardona, A.F., Wilson, S.E., 2015. Skin and soft-tissue infections: a critical review and the role of telavancin in their treatment. *Clin. Infect. Dis.* 61 (Suppl 2), S69–S78. <https://doi.org/10.1093/cid/civ528>.
- Charensriwilaiwat, N., Rojanarat, T., Ngawhirunpat, T., Sukma, M., Opanasopit, P., 2013. Electrospun chitosan-based nanofiber mats loaded with *Garcinia mangostana* extracts. *Int. J. Pharm.* 452 (1–2), 333–343. <https://doi.org/10.1016/j.ijpharm.2013.05.012>.
- Croitoru, A.-M., Ficas, D., Fica, A., Mihailescu, N., Andronescu, E., Turculeț, C.F., 2020. Nanostructured fibers containing natural or synthetic bioactive compounds in wound. *Materials* 13 (2407), 1–19.
- Darie-Niță, R.N., Răpă, M., Fraçkowiak, S., 2022. Special features of polyester-based materials for medical applications. *Polymers* 14 (5), 1–49. <https://doi.org/10.3390/polym14050951>.
- Deng, X., Ali, M.A., Gould, M., 2022. A review of current advancements for wound healing: biomaterial applications and medical devices. *J. Biomed. Mater. Res. B Appl. Biomater.* 1–32. <https://doi.org/10.1002/jbm.b.35086>.
- Dias, J.R., Granja, P.L., Bártolo, P.J., 2016. Advances in electrospun skin substitutes. *Prog. Mater. Sci.* 84, 314–334. <https://doi.org/10.1016/j.pmatsci.2016.09.006>.
- Domingo-Fernández, D., Gadiya, Y., Preto, A.J., Kretzler, C.A., Mubeen, S., Allen, A., Healey, D., Colluru, V., 2024. Natural products have increased rates of clinical trial success throughout the drug development process. *J. Nat. Prod.* 87, 1844–1850. <https://doi.org/10.1021/acs.jnatprod.4c00581>.
- Dorsett-Martin, W.A., 2004. Rat models of skin wound healing: a review. *Wound Repair Regen.* 12 (6), 591–599. <https://doi.org/10.1111/j.1067-1927.2004.12601.x>.
- dos Santos, A.E.A., dos Santos, F.V., Freitas, K.M., Pimenta, L.P.S., de Oliveira Andrade, L., Marinho, T.A., de Avelar, G.F., da Silva, A.B., Ferreira, R.V., 2021. Cellulose acetate nanofibers loaded with crude annatto extract: preparation, characterization, and in vivo evaluation for potential wound healing applications. *Mater. Sci. Eng. C* 118 (November 2019). <https://doi.org/10.1016/j.msec.2020.111322>.
- Eskandarinia, A., Kefayat, A., Gharakhloo, M., Agheb, M., Khodabakhshi, D., Khorshidi, M., Sheikmoradi, V., Rafienia, M., Salehi, H., 2020. A propolis enriched polyurethane-hyaluronic acid nanofibrous wound dressing with remarkable antibacterial and wound healing activities. *Int. J. Biol. Macromol.* 149, 467–476. <https://doi.org/10.1016/j.ijbiomac.2020.01.255>.
- Fahimirad, S., Satei, P., Ganji, A., Abtahi, H., 2023. Wound healing performance of PVA/PCL based electrospun nanofiber incorporated green synthesized CuNPs and *Quercus* infectoria extracts. *J. Biomater. Sci. Polym. Ed.* 34 (3), 277–301. <https://doi.org/10.1080/09205063.2022.2116209>.
- Farahani, H., Barati, A., Arjomandzadegan, M., Vatankhah, E., 2020. Nanofibrous cellulose acetate/gelatin wound dressing endowed with antibacterial and healing efficacy using nanoemulsion of *Zataria multiflora*. *Int. J. Biol. Macromol.* 162, 762–773. <https://doi.org/10.1016/j.ijbiomac.2020.06.175>.
- Fronza, M., Heinzmann, B., Hamburger, M., Laufer, S., Merfort, I., 2009. Determination of the wound healing effect of *Calendula* extracts using the scratch assay with 3T3 fibroblasts. *J. Ethnopharmacol.* 126 (3), 463–467. <https://doi.org/10.1016/j.jep.2009.09.014>.
- Gaaz, T.S., Sulong, A.B., Akhtar, M.N., Kadhum, A.A.H., Mohamad, A.B., Al-Amiery, A. A., McPhee, D.J., 2015. Properties and applications of polyvinyl alcohol, halloysite nanotubes and their nanocomposites. *Molecules* 20 (12), 22833–22847. <https://doi.org/10.3390/molecules201219884>.
- Gama e Silva, G.L., Sato de Souza Bustamante Monteiro, M., dos Santos Matos, A.P., Santos-Oliveira, R., Kenchukwu, F.C., Ricci-Júnior, E., 2022. Nanofibers in the treatment of osteomyelitis and bone regeneration. *J. Drug Delivery Sci. Technol.* 67 (August 2021), 102999. <https://doi.org/10.1016/j.jddst.2021.102999>.
- García-Salinas, S., Gámez, E., Asín, J., De Miguel, R., Andreu, V., Sancho-Albero, M., Mendoza, G., Irusta, S., Arruebo, M., 2020. Efficiency of antimicrobial electrospun thymol-loaded polycaprolactone mats in vivo. *ACS Appl. Bio Materials* 3 (5), 3430–3439. <https://doi.org/10.1021/acsbm.0c00419>.
- Gasparetto, J.C., Martins, C.A.F., Hayashi, S.S., Otuky, M.F., Pontarolo, R., 2012. Ethnobotanical and scientific aspects of *Malva sylvestris* L.: a millennial herbal medicine. *J. Pharm. Pharmacol.* 64 (2), 172–189. <https://doi.org/10.1111/j.2042-7158.2011.01383.x>.
- Ghosh, P.K., Gaba, A., 2013. Phyto-extracts in wound healing. *J. Pharm. Pharm. Sci.* 16 (5), 760–820. <https://doi.org/10.18433/j3831v>.
- Goher, S.S., Aly, S.H., Abu-Serie, M.M., El-Moslami, S.H., Allam, A.A., Diab, N.H., Hassanein, K.M.A., Eissa, R.A., Eissa, N.G., Elsbahy, M., Kamoun, E.A., 2024. Electrospun *Tamarindus indica*-loaded antimicrobial PMMA/cellulose acetate/PEO nanofibrous scaffolds for accelerated wound healing: in-vitro and in-vivo assessments. *Int. J. Biol. Macromol.* 258 (August 2023). <https://doi.org/10.1016/j.ijbiomac.2023.128793>.
- Grada, A., Mervis, J., Falanga, V., 2018. Research techniques made simple: animal models of wound healing. *J. Invest. Dermatol.* 138 (10), 2095–2105.e1. <https://doi.org/10.1016/j.jid.2018.08.005>.
- Gupta, P., Mishra, P., Mehra, L., Rastogi, K., Prasad, R., Mittal, G., Poluri, K.M., 2021. Eugenol-acacia gum-based bifunctional nanofibers as a potent antifungal transdermal substitute. *Nanomedicine* 16 (25), 2269–2289. <https://doi.org/10.2217/nnm-2021-0274>.
- Hajialyani, M., Tewari, D., Sobarzo-Sánchez, E., Nabavi, S.M., Farzaei, M.H., Abdollahi, M., 2018. Natural product-based nanomedicines for wound healing purposes: therapeutic targets and drug delivery systems. *Int. J. Nanomed.* 13, 5023–5043. <https://doi.org/10.2147/IJN.S174072>.
- Han, G., Ceilley, R., 2017. Chronic wound healing: a review of current management and treatments. *Adv. Ther.* 34 (3), 599–610. <https://doi.org/10.1007/s12325-017-0478-y>.
- Harris-Tryon, T.A., Grice, E.A., 2022. Microbiota and maintenance of skin barrier function. *Science* 376 (6596), 940–945. <https://doi.org/10.1126/science.abo0693>.
- Hatlen, T.J., Miller, L.G., 2021. Staphylococcal skin and soft tissue infections. *Infect. Dis. Clin. North Am.* 35 (1), 81–105. <https://doi.org/10.1016/j.idc.2020.10.003>.
- Irani, M., Abadi, P.G.S., Ahmadian-Attari, M.M., Rezaee, A., Kordbacheh, H., Goleij, P., 2024. In vitro and in vivo studies of *Dragon's blood plant* (*D. cinnabari*)-loaded electrospun chitosan/PCL nanofibers: cytotoxicity, antibacterial, and wound healing activities. *Int. J. Biol. Macromol.* 257 (December 2023). <https://doi.org/10.1016/j.ijbiomac.2023.128634>.
- Islam, M.M., Ramesh, V.H., Bhavani, P.D., Goudanavar, P.S., Naveen, N.R., Ramesh, B., Fattepur, S., Narayanappa Shiroorkar, P., Habeebuddin, M., Meravanige, G., Telsang, M., Sreeharsha, N., 2022. Optimization of process parameters for fabrication of electrospun nanofibers containing neomycin sulfate and Malva sylvestris extract for a better diabetic wound healing. *Drug Deliv.* 29 (1), 3370–3383. <https://doi.org/10.1080/10717544.2022.2144963>.
- Jabbour, J.F., Kanj, S.S., 2021. Gram-negative skin and soft tissue infections. *Infect. Dis. Clin. North Am.* 35 (1), 157–167. <https://doi.org/10.1016/j.idc.2020.10.008>.
- Kalachaveedu, M., Jenifer, P., Pandian, R., Arumugam, G., 2020. Fabrication and characterization of herbal drug enriched Guar galactomannan based nanofibrous mats seeded with GMSC's for wound healing applications. *Int. J. Biol. Macromol.* 148, 737–749. <https://doi.org/10.1016/j.ijbiomac.2020.01.188>.
- Ke, M., Wang, Z., Dong, Q., Chen, F., He, L., Huselstein, C., Wang, X., Chen, Y., 2021. Facile fabrication of soy protein isolate-functionalized nanofibers with enhanced biocompatibility and hemostatic effect on full-thickness skin injury. *Nanoscale* 13 (37), 15743–15754. <https://doi.org/10.1039/d1nr03430h>.
- Keirouz, A., Chung, M., Kwon, J., Fortunato, G., Radaci, N., 2020. 2D and 3D electrospinning technologies for the fabrication of nanofibrous scaffolds for skin tissue engineering: a review. *Wiley Interdiscip. Rev. Nanomed. Nanobiotechnol.* 12 (4), 1–32. <https://doi.org/10.1002/wnan.1626>.
- Kharat, Z., Amiri Goushki, M., Sarvian, N., Asad, S., Dehghan, M.M., Kabiri, M., 2021. Chitosan/PEO nanofibers containing *Calendula officinalis* extract: preparation, characterization, in vitro and in vivo evaluation for wound healing applications. *Int. J. Pharm.* 609 (September), 121132. <https://doi.org/10.1016/j.ijpharm.2021.121132>.
- Kilkenny, C., Browne, W.J., Cuthill, I.C., Emerson, M., Altman, D.G., 2010. Improving bioscience research reporting: the ARRIVE guidelines for reporting animal research. *J. Pharmacol. Pharmacother.* 1 (2), 94–99. <https://doi.org/10.4103/0976-500x.72351>.

- Li, Y., Meng, Q., Chen, S., Ling, P., Kuss, M.A., Duan, B., Wu, S., 2023. Advances, challenges, and prospects for surgical suture materials. *Acta Biomater.* 168, 78–112. <https://doi.org/10.1016/j.actbio.2023.07.041>.
- Li, T., Sun, M., Wu, S., 2022. State-of-the-art review of electrospun gelatin-based nanofiber dressings for wound healing applications. *Nanomaterials* 12 (784).
- Li, Y., Zhao, W., Chen, S., Zhai, H., Wu, S., 2024. Bioactive electrospun nanoyarn-constructed textile dressing patches delivering Chinese herbal compound for accelerated diabetic wound healing. *Mater. Des.* 237 (August 2023). <https://doi.org/10.1016/j.matdes.2023.112623>.
- Meng, Q., Li, Y., Wang, Q., Wang, Y., Li, K., Chen, S., Ling, P., Wu, S., 2024. Recent advances of electrospun nanofiber-enhanced hydrogel composite scaffolds in tissue engineering. *J. Manuf. Process.* 123 (June), 112–127. <https://doi.org/10.1016/j.jmapro.2024.05.085>.
- Mirhaj, M., Varshosaz, J., Nasab, P.M., Al-Musawi, M.H., Almajidi, Y.Q., Shahriari-Khalaji, M., Tavakoli, M., Alizadeh, M., Sharifianjazi, F., Mehrjoo, M., Labbaf, S., Sattar, M., Esfahani, S.N., 2024. A double-layer cellulose/pectin-soy protein isolate-pomegranate peel extract micro/nanofiber dressing for acceleration of wound healing. *Int. J. Biol. Macromol.* 255 (September 2023). <https://doi.org/10.1016/j.ijbiomac.2023.128198>.
- Nano4Fibers, 2023. *Nano4Fibers products*. <https://www.nano4fibers.com/we-sell>.
- NanoLayr, 2023. *Dermalayr*. <https://www.nanolayr.com/product/dermalayr/>.
- Nayak, B.S., Isitor, G., Davis, E.M., Pillai, G.K., 2007. The evidence based wound healing activity of Lawsonia inermis Linn. *Phytother. Res.* 21, 827–831 doi: 10.1002/ptr.
- Nejaddehbashi, F., Rafiee, Z., Orazizadeh, M., Bayati, V., Hemmati, A., Hashemitabar, M., Makvandi, P., 2023. Antibacterial and antioxidant double-layered nanofibrous mat promotes wound healing in diabetic rats. *Sci. Rep.* 13 (1), 1–15. <https://doi.org/10.1038/s41598-023-30240-8>.
- Nemati, D., Ashjari, M., Rashedi, H., Yazdian, F., Navaei-Nigjeh, M., 2021. PVA based nanofiber containing cellulose modified with graphitic carbon nitride/nettles/trachyspermum accelerates wound healing. *Biotechnol. Prog.* 37 (6). <https://doi.org/10.1002/btpr.3200>.
- Neotherix, 2023. *Neotherix products*. <https://www.neotherix.com/products/>.
- Newman, D.J., Cragg, G.M., 2012. Natural products as sources of new drugs over the 30 years from 1981 to 2010. *J. Nat. Prod.* 75, 311–335. <https://doi.org/10.1021/acs.jnatprod.5b01055>.
- Newman, D.J., Cragg, G.M., 2020. Natural products as sources of new drugs over the nearly four decades from 01/1981 to 09/2019. *J. Nat. Prod.* 83 (3), 770–803. <https://doi.org/10.1021/acs.jnatprod.9b01285>.
- Pereira, R.F., Bártolo, P.J., 2016. Traditional therapies for skin wound healing. *Adv. Wound Care* 5 (5), 208–229. <https://doi.org/10.1089/wound.2013.0506>.
- Riss, T.L., Moravec, R.A., Niles, A.L., Duellman, S., Benink, H.A., Worzella, T.J., Minor, L., 2004. Cell viability assays. *Assay Guidance Manual*, Md 1–25.
- Salami, M.S., Bahrami, G., Arkan, E., Izadi, Z., Miraghaee, S., Samadian, H., 2021. Co-electrospun nanofibrous mats loaded with bitter melon (*Momordica charantia*) extract as the wound dressing materials: in vitro and in vivo study. *BMC Complement. Med. Therap.* 21 (1), 1–12. <https://doi.org/10.1186/s12906-021-03284-4>.
- Sarhan, W.A., Azzazy, H.M., 2017. Apitherapeutics and phage-loaded nanofibers as wound dressings with enhanced wound healing and antibacterial activity. *Nanomedicine* 12 (17), 2055–2067. <https://doi.org/10.2217/nnm-2017-0151>.
- Scepankova, H., Combarros-Fuertes, P., Fresno, J.M., Tornadajo, M.E., Dias, M.S., Pinto, C.A., Saraiva, J.A., Esteveinho, L.M., 2021. Role of honey in advanced wound care. *Molecules* 26 (16), 1–19. <https://doi.org/10.3390/molecules26164784>.
- Selvakumar, P.M., Rajkumar, S., R., J., Msa, M.N., 2018. Phytochemicals as a potential source for anti-microbial, anti-oxidant and wound healing – a review. *MOJ Bioorg. Org. Chem.* 2 (2). <https://doi.org/10.15406/mojboc.2018.02.0058>.
- Sharaf, S.M., Al-Mofly, S.E.D., El-Sayed, E.S.M., Omar, A., Abo Dena, A.S., El-Sherbiny, I. M., 2021. Deacetylated cellulose acetate nanofibrous dressing loaded with chitosan/propolis nanoparticles for the effective treatment of burn wounds. *Int. J. Biol. Macromol.* 193 (PB), 2029–2037. <https://doi.org/10.1016/j.ijbiomac.2021.11.034>.
- Simões, D., Miguel, S.P., Ribeiro, M.P., Coutinho, P., Mendonça, A.G., Correia, I.J., 2018. Recent advances on antimicrobial wound dressing: a review. *Eur. J. Pharm. Biopharm.* 127 (February), 130–141. <https://doi.org/10.1016/j.ejpb.2018.02.022>.
- Solutions, N., 2023. *3D-Cell Culture Nanofiber Solutions*. <https://nanofibersolutions.com/product-category/3d-cell-culture/>.
- Sorg, H., Sorg, C.G.G., 2023. Skin wound healing: of players, patterns, and processes. *Eur. Surg. Res.* 64 (2), 141–157. <https://doi.org/10.1159/000528271>.
- Supino, R., 1995. MTT assays. *Methods Mol. Biol. (Clifton, N.J.)* 43, 137–149. <https://doi.org/10.1385/0-89603-282-5:137>.
- Tahami, S.R., Nemati, N.H., Keshvari, H., Khorasani, M.T., 2022. In vitro and in vivo evaluation of nanofibre mats containing *Calendula officinalis* extract as a wound dressing. *J. Wound Care* 31 (7), 598–611. <https://doi.org/10.12968/jowc.2022.31.7.598>.
- Terezaki, A., Kikionis, S., Ioannou, E., Sfiriadakis, I., Tziveleka, L.A., Vitsos, A., Roussis, V., Rallis, M., 2022. Ulvan/gelatin-based nanofibrous patches as a promising treatment for burn wounds. *J. Drug Delivery Sci. Technol.* 74 (June), 103535. <https://doi.org/10.1016/j.jddst.2022.103535>.
- Wang, Q., Zhang, S., Jiang, J., Chen, S., Ramakrishna, S., Zhao, W., Yang, F., Wu, S., 2024. Electrospun radially oriented berberine-PHBV nanofiber dressing patches for accelerating diabetic wound healing. *Regener. Biomater.* 11 (June). <https://doi.org/10.1093/rb/rbae063>.
- Wu, S., Dong, T., Li, Y., Sun, M., Qi, Y., Liu, J., Kuss, M.A., Chen, S., Duan, B., 2022. State-of-the-art review of advanced electrospun nanofiber yarn-based textiles for biomedical applications. *Appl. Mater. Today* 27. <https://doi.org/10.1016/j.apmt.2022.101473>.
- Yang, Y., Qu, L., Mijakovic, I., Wei, Y., 2022. Advances in the human skin microbiota and its roles in cutaneous diseases. *Microb. Cell Fact.* 21 (1), 1–14. <https://doi.org/10.1186/s12934-022-01901-6>.
- Yao, C.H., Chen, K.Y., Chen, Y.S., Li, S.J., Huang, C.H., 2019. Lithospermi radix extract-containing bilayer nanofiber scaffold for promoting wound healing in a rat model. *Mater. Sci. Eng. C* 96, 850–858. <https://doi.org/10.1016/j.msec.2018.11.053>.
- Yousefi, I., Pakravan, M., Rahimi, H., Bahador, A., Farshadzadeh, Z., Haririan, I., 2017. An investigation of electrospun Henna leaves extract-loaded chitosan based nanofibrous mats for skin tissue engineering. *Mater. Sci. Eng. C* 75, 433–444. <https://doi.org/10.1016/j.msec.2017.02.076>.
- Zeus, 2023. *Bioweb Zeus*. <https://www.zeusinc.com/products/biomaterials/bioweb-composites>.
- Zwierzyzna, M., Overington, J.P., 2017. Classification and analysis of a large collection of in vivo bioassay descriptions. *PLoS Comput. Biol.* 13 (7). <https://doi.org/10.1371/journal.pcbi.1005641>.